DYNAMIC TESTS OF A THREE-SPAN CONTINUOUS I-BEAM HIGHWAY BRIDGE

Final Report

by

C. L. Hulsbos, Professor of Civil Engineering
and
D. A. Linger, Instructor of Civil Engineering

Iowa Highway Research Project HR-43

October, 1959

Project 334-S

Iowa Engineering Experiment Station
Iowa State University
Ames, Iowa

CONTENTS

ABSTRACT

This paper presents the results of the static and dynamic testing of a three-span continuous I-beam highway bridge. Live load stress frequency curves for selected points are shown, and the static and dynamic load distribution to the longitudinal composite beam members are given.

The bridge has four traffic lanes with a roadway width of 48 ft. Six longitudinal continuous WF beams act compositely with the reinforced concrete slab to carry the live load. The beams have partial length cover plates at the piers.

Previous research has indicated that beams with partial length cover plates have a very low fatigue strength. It was found in this research that the magnitude of the stresses due to actual highway loads were very much smaller than those computed from specification loading. Also, the larger stresses which were measured occurred a relatively small number of times. These data indicate that some requirements for reduced allowable stresses at the ends of cover plates are too conservative.

The load distribution to the longitudinal beams was determined for static and moving loads and includes the effect of impact on the distribution. The effective composite section was found at various locations to evaluate the load distribution data. The composite action was in negative as well as positive moment regions. The load distribution data indicate that the lateral distribution of live load is consistent with the specifications but that there is longitudinal distribution, and therefore the specifications are too conservative.

INTRODUCTION

In 1944 the first specifications for the design of composite highway bridges were published as a part of the American Association of State Highway Officials "Standard Specifications". The acceptance of this type of construction is shown by the increased use of composite steel and concrete in highway bridges. The resulting bridge structure is lighter and has a larger span depth ratio than ever before.

In the composite steel stringer bridge with a reinforced concrete slab, the roadway slab is used not only to transfer the load laterally, but also to form a composite section in conjunction with the longitudinal steel stringers. Therefore the slab adds not only lateral stiffness but also considerably to the basic longitudinal load carrying capacity of the stringers. Thus, the steel stringer can be reduced considerably in size with a saving in both dead load and the cost of the structure. In addition, the reduction in dead load allows the basic superstructure to be decreased in size, resulting in a much lighter bridge.

Additional reduction in the size of the steel stringers can be obtained if the structure is made continuous over a number of supports. This continuity tends to increase the ultimate load carrying capacity of the bridge structure. This is an aspect which should be considered because of loading at some future time, which might produce an extreme overload on the bridge.

However, some problems arise when the stringer is made continuous. The most significant is that the "Standard Specifications" do not permit the use of composite action in the area of negative moments. Since composite action is not accepted, cover plates must be added to the longitudinal

stringers along some portion of this negative moment region.

Recent results of fatigue tests of rolled beams with cover plates indicate that fatigue might be critical in the life of this type of structure[1]. Fatigue life depends both on the level of the stress and on stress repetition: i.e. the level of the stress during the reversal or cycle of the stress repetition. It can be shown that with specification loading, stress reversals at the ends of the cover plates are large enough to cause fatigue failure after the required number of reversals. However, these computed stresses may be erroneous, since many assumptions, mainly those of load distribution and impact, are made in their calculations.

The problem of fatigue is acute because of the dynamic behavior of a continuous type of bridge. This behavior, usually vibration, is a result of the large span depth ratio. Its consequence is not only increased stress, which is usually within the impact factor, but also the repetition of this stress resulting from prolonged vibration.

A recent survey [2] shows that over half the state highway departments in this country are using rolled beams with partial length cover plates to some extent. These state highway commissions use various types of cover plate termination details. These end details have an important effect on the fatigue strength of rolled sections with partial length cover plates.

The Iowa State Highway Commission is now using a cover plate termination detail with a rectangular end which is tapered and welded along its entire end. However, a type of cover plate termination detail previously used in Iowa was investigated in this research because it was considered more conducive to stress concentration than the present detail (figure 4a).

OBJECTIVES

The objective of this research is to determine experimentally the live load stresses in the cover plate termination region, and to determine the stress frequency curves for in-service loading. Once these stress-frequency curves are determined, laboratory tests may be designed to use these fatigue data in determining the permissable stress for the cover plate cutoff points.

Although it was not the intent of this research to evaluate load distribution to the longitudinal stringers, this is inherent any time an experimental stress is compared with a theoretical stress. As a part of the load distribution problem, the vibration characteristics and composite section properties were studied. Therefore, the problem of load distribution is an objective of this research, though an indirect one.

STRAIN EQUIPMENT

The objectives of this research required not only that the magnitude of the stress be determined but also that a complete stress-time curve be constructed for the passage of each vehicle over the bridge. In other words, an instrument was required which could record the stresses continuously over an extended period of time.

The term stress analysis is inaccurate, because although we speak of measuring stresses we actually must measure strains and convert these to stresses. Of the many varied ways of measuring strains, the requirement of a continuous record of strain dictated the type of strain gage and limited the variation in types of strain recorders.

To measure the strains, standard SR-4 strain gages, which can be applied with a minimum amount of work were used. The beams are pre-

pared by removing paint and scale, and then the gages are attached with a special air-drying cement. This type of strain gage measures the strain by the amount of change in resistance of a small diameter wire located in the gage immediately adjacent to the beam. The advantages of this type of strain gage are the small mass of the gage itself and the direct method of attaching, which does not have any mechanical parts and requires no alteration of the structure. This type of gage should indicate the exact strain to be recorded, whether or not there is acceleration present in the structure at the time the strain is recorded. This is important because the investigation required that the stresses resulting from the dynamic loads be recorded without any distortion from within the gage itself. The types of SR-4 gages used were A-11 and A-5. The resistance to the ground of the SR-4 gages were as follows: The A-11 gages 50,000 to 100,000 ohms; the A-5 1000,000 to 1,000,000 ohms.

The strain readings were recorded by a Brush universal amplifier (BL-520) and a Brush direct-writing recorder (BL-274). This equipment produces a continuous record of strain for which the time base can be varied by the speed of the recording paper. The speeds available vary from 1 to 250 mm/sec. For a check of the time base as determined by the speed of the paper, a one second timer was used to actuate an event marker on the edge of the record. The Brush Universal amplifiers have a number of attenuator settings which vary from 1 microinch/inch of strain/Attenuator-Line to 1000 microinch/inch of strain/Attenuator-Line, and therefore allow a wide choice of amplification of the strain to best utilize the recording paper.

THE STRUCTURE

The test bridge was selected because of its location, accessibility, and its similarity to the type of bridge currently being built in Iowa's primary road system (figure 1). The bridge is located on U.S. Highway 30 one mile east of Ames, Iowa. Highway 30 crosses the Skunk River at this point, and the bridge is often referred to as the "Skunk River" bridge. The structure has longitudinal steel wide-flange supporting stringers constructed integrally with a reinforced concrete slab roadway. Shear lugs were provided to ensure composite action between the stringers and the concrete roadway slab. The steel diaphrams are spaced at 18 ft., 6 in. $\pm$ 3 in. centers. The bridge has four 12 ft. lanes and a 2 ft. safety curb on both sides.

THE LOADINGS

CONTROLLED LOAD

Two types of loading were necessary for the data required. The first type was a standard controlled load needed to evaluate the load distribution and impact stresses. This loading was used also to evaluate the stress distribution around the cover plate termination area. The vehicle used in this loading is a tandem axle, International L-190 van type truck (figure 2). This truck used to check the Iowa State Highway Commission scales, has a wheel base of 14 ft., 8 in. and a tread of 6 ft. It weighs 40,650 lbs with 31,860 lbs on the rear axle. The standard truck was used to evaluate the distribution of the load to the various stringers and the amount of the increase in stress due to impact. This information was obtained by running the loading vehicle at different speeds across the bridge at different locations on the bridge roadway profile.

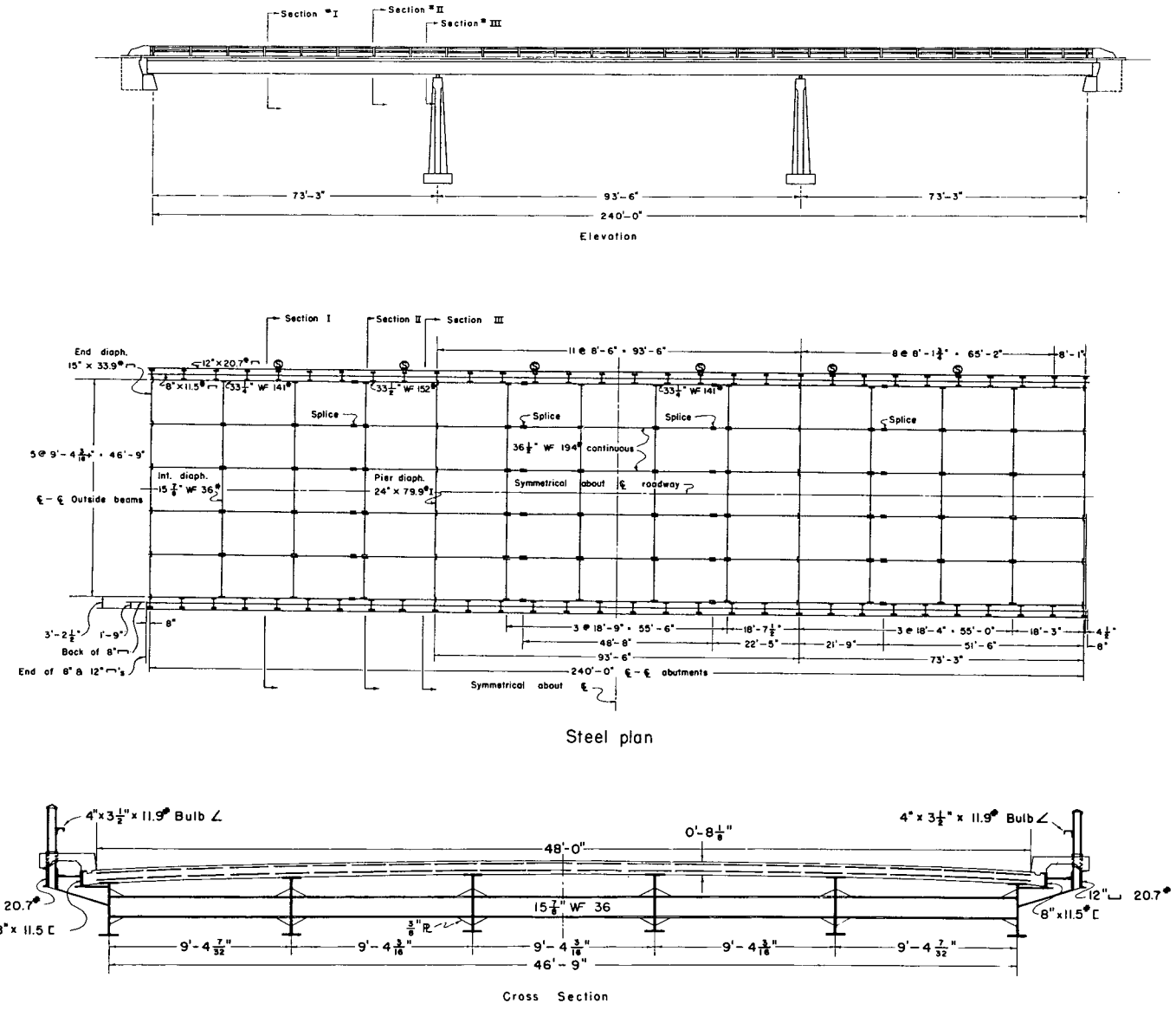

Figure 1. Elevation, plan, and cross section of the test bridge.

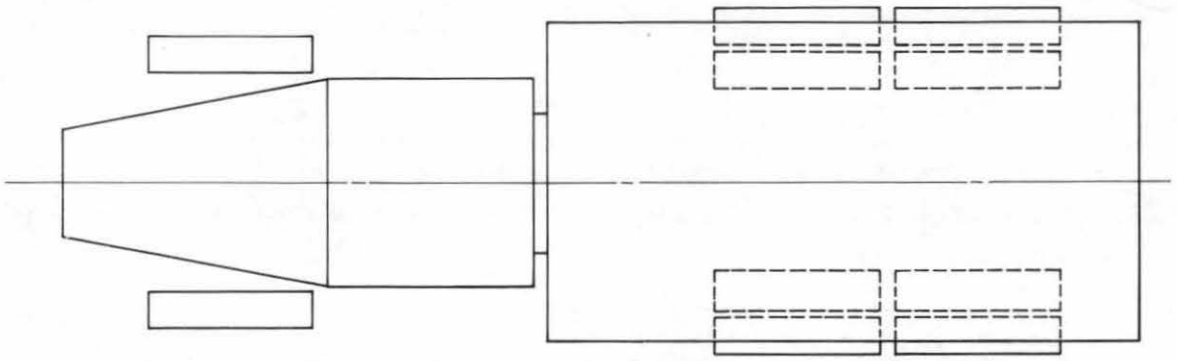

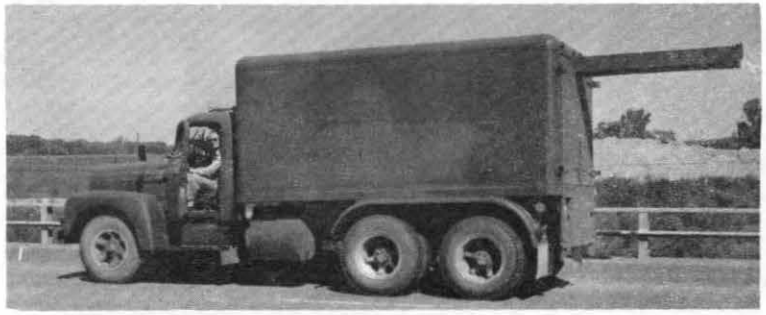

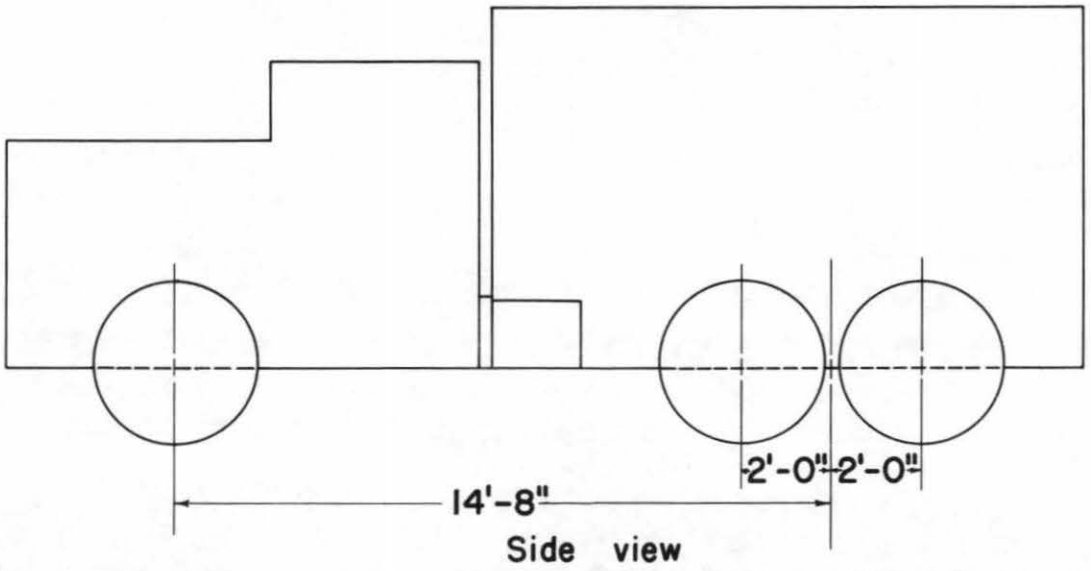

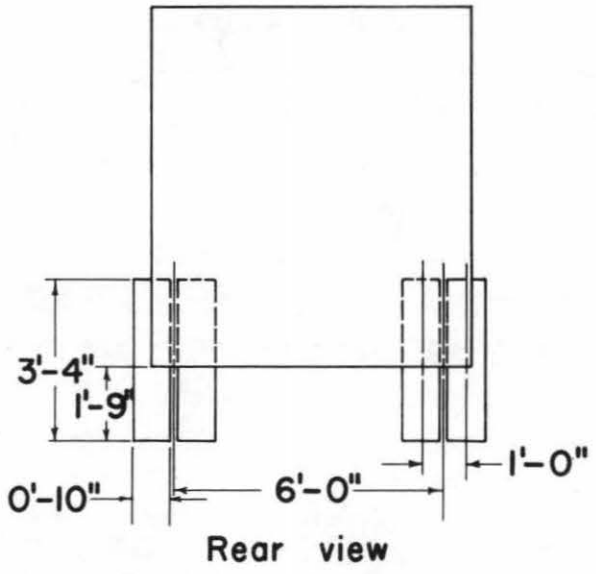

Figure 2. The standard (H-20) loading vehicle.

Fourteen different "lanes" were marked on the bridge roadway (figure 3). These "lanes" overlapped three feet.

The "static" tests were performed by the controlled loading vehicle creeping across the bridge with the motor idling. This loading was performed on all fourteen test "lanes" of the bridge. The moving load tests were conducted at vehicle speeds beginning at 10 mph. and increasing by approximately 10 mph. increments up to the maximum attainable speed of approximately 50 mph. The maximum speed was limited by the vehicle and the terrain. These moving load tests were conducted on only four of the fourteen test "lanes". The speed of the test vehicle was determined by two air hose switches connected to a speed indicator on the roadway at one end of the structure. The indicator is the property of the Safety Department of the Iowa State Highway Commission. During the moving load tests, the vehicle's speed was constant over the entire length of the bridge, and the vehicle did not vary from the assigned "lane". Each of the fourteen "lanes" used was marked by a painted stripe along which the left front tire of the truck was run. During the speed runs the variation to one side or the other of the vehicle was never more than one and a half inches.

RANDOM LOAD

For the random load test the actual in-service traffic was recorded. In this traffic were trucks, semi-trucks, buses, cars, and miscellaneous vehicles. The stresses resulting from this traffic were recorded, and the type, direction, and highway lane-of-travel of the vehicles were noted on the record. The record was run for a period of four hours a day for two days. The operating periods were staggered so that the two four hour periods together covered a period from 10:00 A.M. to 5:30 P.M.

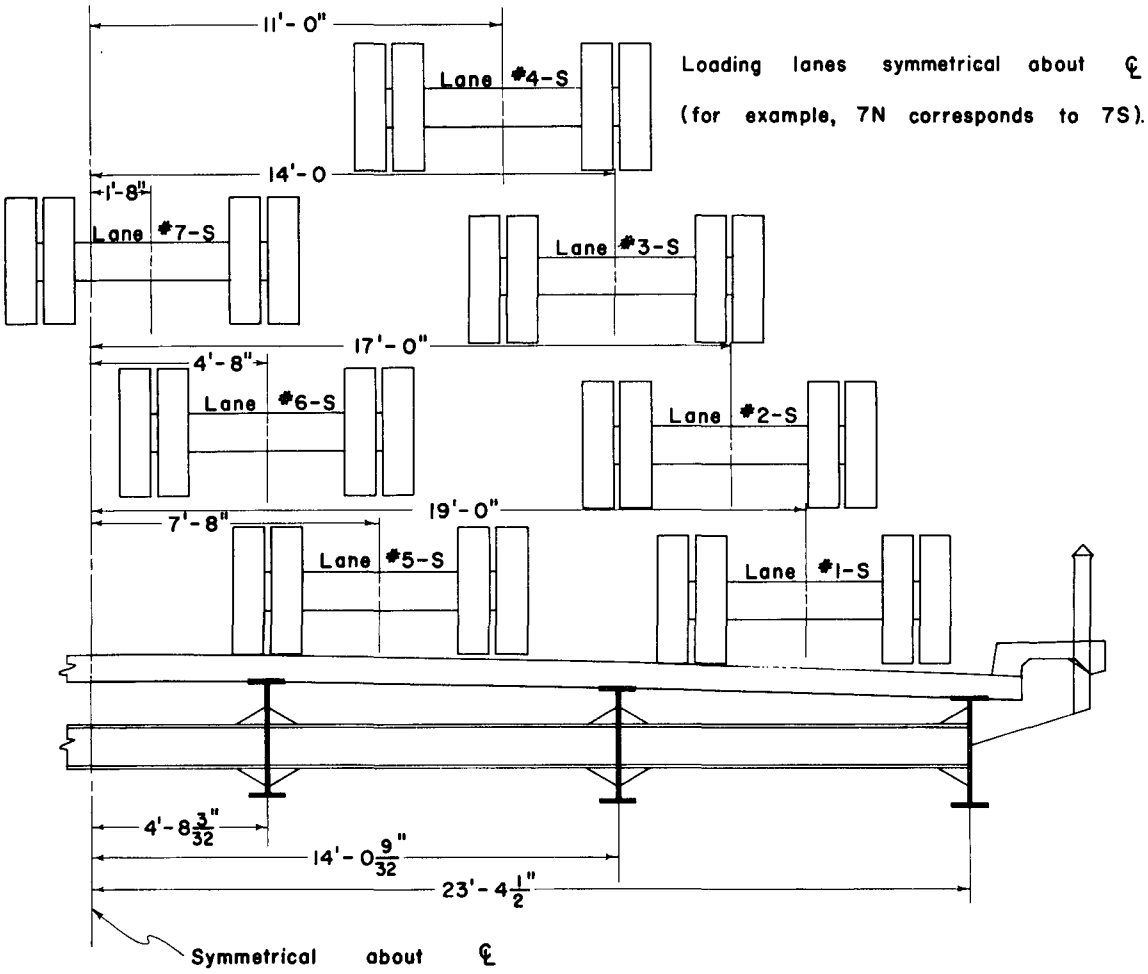

Figure 3. Cross section showing 14 "lanes".

TEST RESULTS

STRESS DISTRIBUTION IN THE COVER PLATE TERMINATION AREA

The distribution of stress in the cover plate termination region was determined first. This was required so that a location could be established for an indicator gage which would yield repeatable results, would not be affected by stress raisers, and could be correlated with the stresses at points of stress concentration.

Figure 4b and 4c show the longitudinal stress variation as contour lines on the cover plate termination area. These lines were constructed by assuming that the strain varied linearly between the nineteen strain gage locations used. This is, of course, an approximation, but it gives an indication of the variation of the stresses. This approximate anomaly picture was used only to determine the best place for the single strain gage. This gage was used as an indicator for each cover plate termination area for the measurement of the strains during the moving load tests. This point was chosen because a center line location was desirable due to the symmetry of the detail. The distance from the end of the cover plate is large enough that the strain measured is not at the point of maximum stress concentration and yet close enough to indicate the response of the cover plate termination detail to various moving loads.

The location chosen for the individual gage was 2 1/2 inches away from the end of the cover plate along the center line of the flange. All the cover plate termination areas in one quadrant of the bridge plan were instrumented with a single gage located at that point. This particular point is indicated in figure 4 by 100%, since it was used as a base for the percentage contour line.

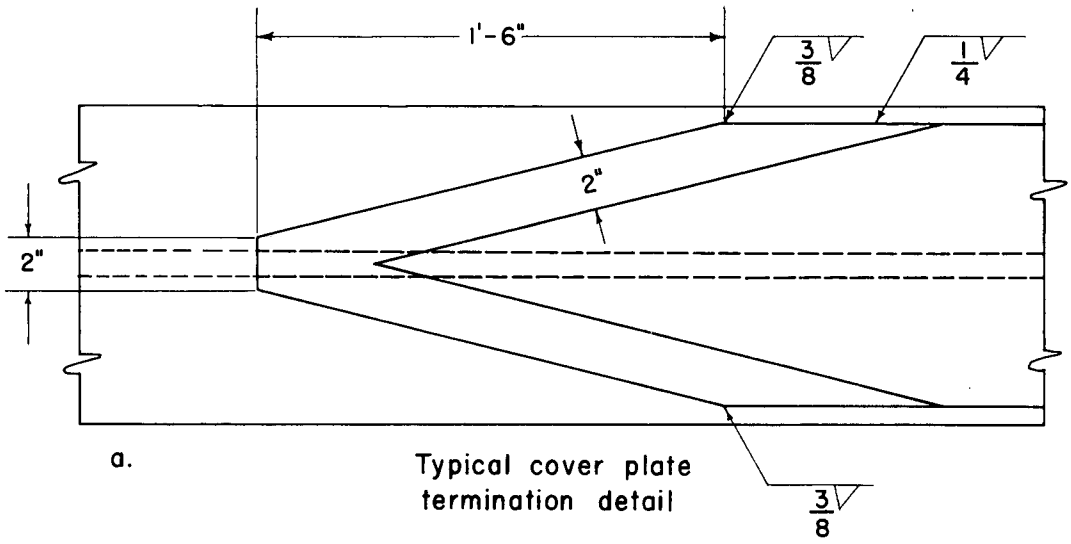

a. Typical cover plate termination detail

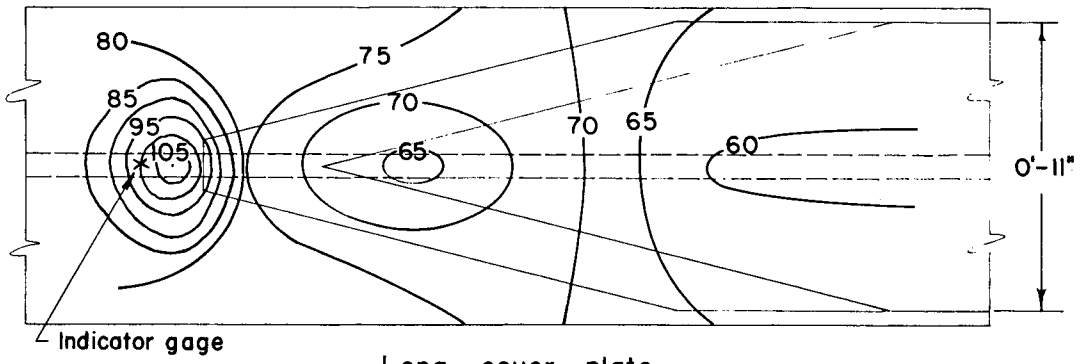

b. Long cover plate

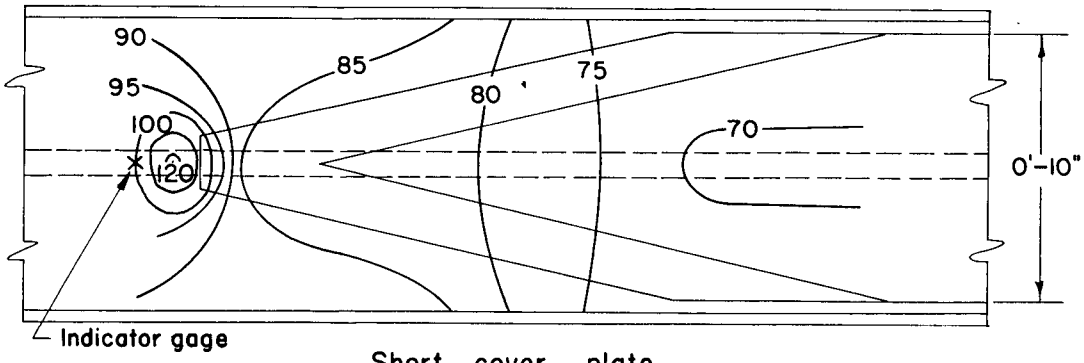

c. Short cover plate

Figure 4. Typical cover plate termination detail (at top), and longitudinal stress contours.

STRESS FREQUENCY CURVES

The stress history of a structure can be shown best by a continuous record of stress measured over a period of time. This picture of the stress variations is, however, not satisfactory for the most concise indication of the susceptibility of a structure to fatigue. The factors affecting fatigue are the intensity of stress and the number of times this stress is repeated. Therefore, the stress history of a structure, from the fatigue aspect, is most easily shown by a stress frequency curve. The data for this curve is obtained from a continuous strain record.

A typical continuous strain record curve shows the variation of strain as a vehicle passes over the structure (figure 5). To construct a stress-frequency curve from this record, the number of times the strain record exceeds each stress level in the rising direction is plotted on the abscissa of the stress-frequency diagram (figure 6).

The Random Traffic

To obtain the in-service stress history of the cover plate termination areas, which was the primary objective of this research, a continuous record of strain was obtained for a given period of time. Once this was obtained the stress-frequency curves for this traffic were constructed to show the cyclical stress repetition occurring in these areas of potential fatigue failures. These stress-frequency curves or stress histories of the traffic sampled, show the susceptibility of the cover plate termination region to fatigue failure under in-service conditions. The data for this information were obtained by recording the strain at the "indicator" gages located 2 1/2 inches from the end of the long cover plates in one quadrant of the bridge plan. Thus because of bi-lateral and bi-longitudinal symmetry the strains recorded are typical of all the long cover-plate termination regions of this structure.

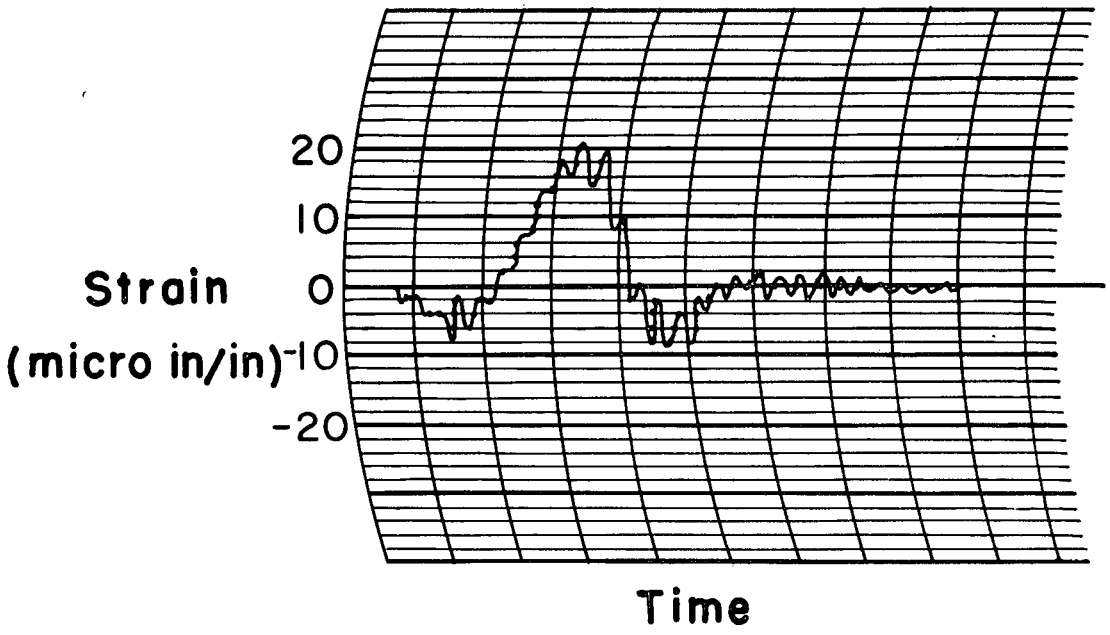

Figure 5. Typical continuous strain record.

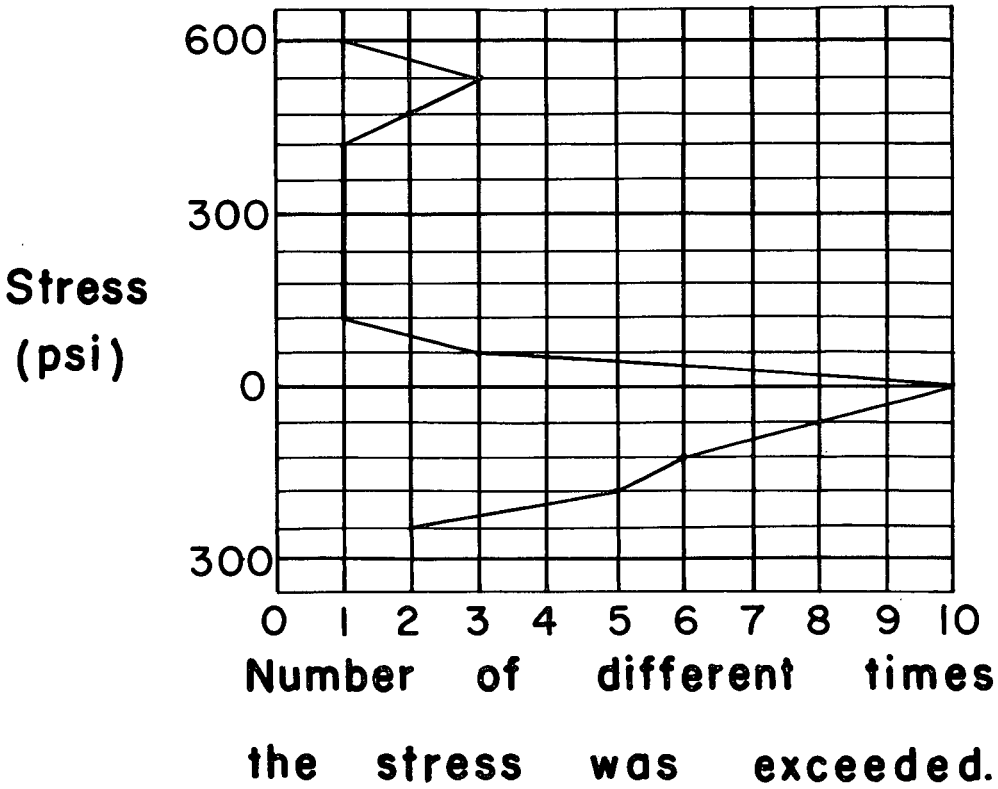

Figure 6. Stress frequency curve for typical strain record.

The random traffic sampled was typical mid-week primary road traffic. The sample was obtained on the morning of Tuesday, July 29, and the afternoon of Wednesday, July 30, 1958. The time factor for the random samples is equivalent to 7 1/2 hours of continuous sampling from 10:00 A.M. to 5:30 P.M. In terms of the number of vehicles the sample is the result of 253 vehicles which includes semi-trucks, conventional single-unit trucks, and busses.

The average maximum strain produced by individual automobiles traveling across the bridge was approximately five micro in/in, this is less than 1/10 of the average maximum strain produced by trucks and busses. Because of the small strain produced by individual automobiles this strain was insignificant in its effect on the fatigue life of the bridge. Therefore, the stress frequency curves in figure 7 include only the trucks and busses and combination of automobiles with trucks and busses and are incomplete in the range of $\pm$ 5 micro in/in, or $\pm$ 150 psi.

Only when an automobile was immediately preceeded by a large truck, especially a semi-truck, was the strain produced by an automobile significant. The vibratory motion produced by the truck was often amplified by the automobile, but in most cases the automobile only caused the vibration to continue for a longer period at the same amplitude as that produced by the truck. The period of this bridge vibration is 0.313 seconds. This frequency of vibration was often superimposed in a slower vibration of 3.4 seconds (figure 8). This "beat" or superposition of two frequencies resulted usually in the stringers which are not directly below the load, but adjacent to the "loaded" stringer. The vibration which results from this "beat" causes rather large strains, which are repeated an average of thirty times during the course of the vibration caused by one truck.

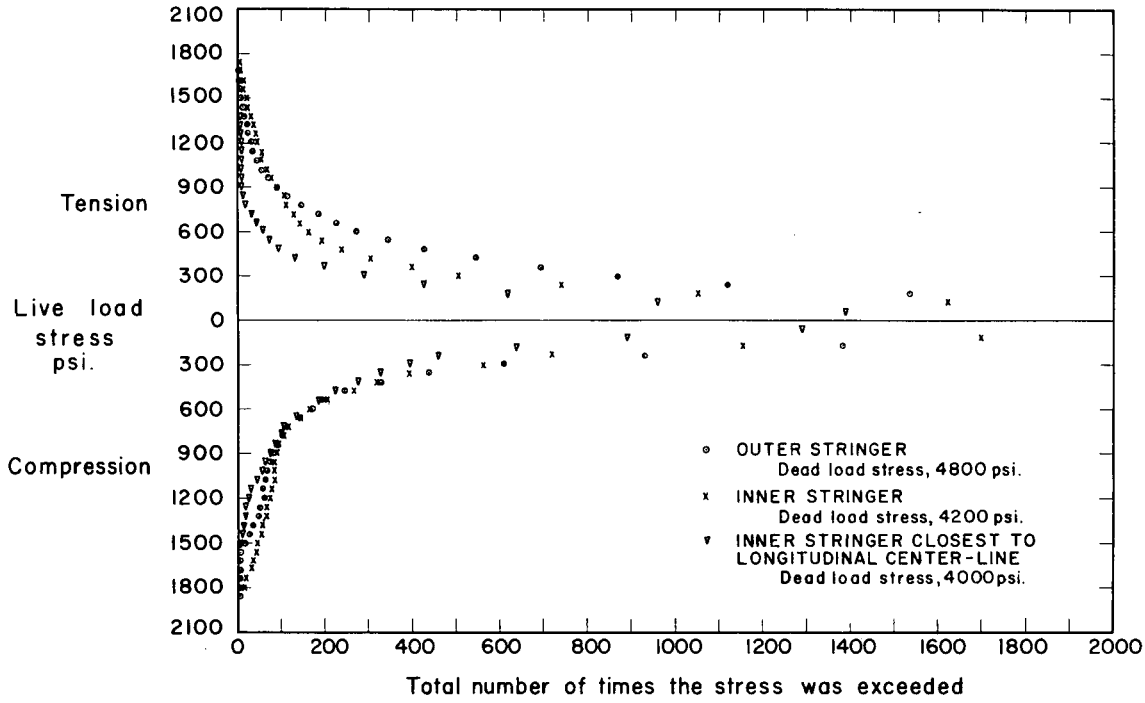

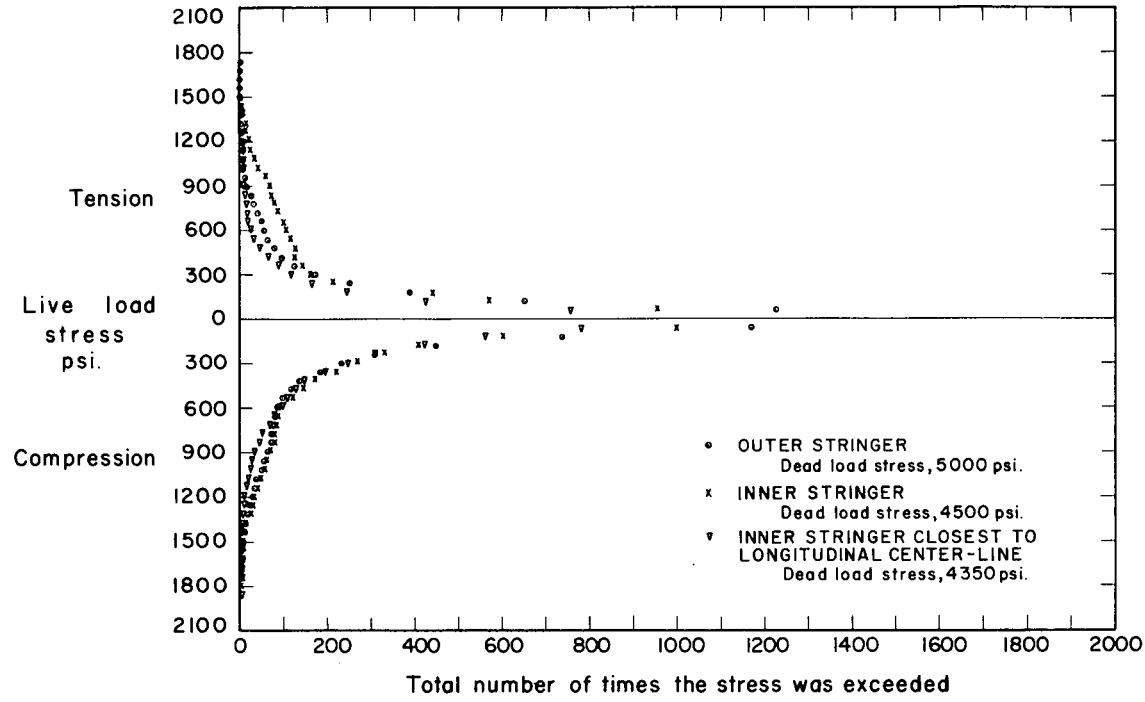

Figure 7. Stress frequency curves for the end span (at top) and stress frequency curves for the center span.

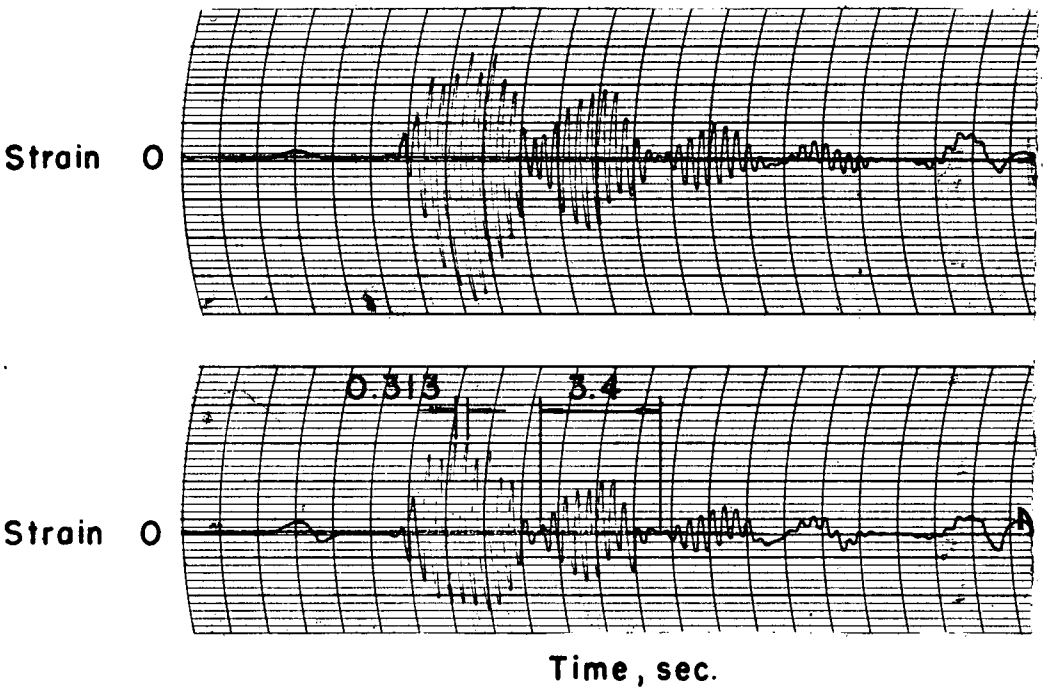

Figure 8. Beat frequency vibration due to moving loads.

The largest strain recorded was 60 micro in/in, which corresponds to stress of 1,800 psi. This stress was not repeated more than nine times during the 7 1/2 hours of strain recording. This stress is, of course, in addition to the dead load stress which varies between 4,000 and 5,000 psi for the stringers subjected to this maximum repeated live load stress. The dead load stresses are shown for each different cover plate cut-off point as the equilibrium or zero live load stress ordinate on the stress-frequency diagrams (figure 7). The cut-off design stress for the test bridge cover plates are based on the equation

$$fs = 18{,}000 - 5\left(\frac{L}{b}\right)^2$$

This equation yields an allowable stress of 16,190 psi for the outer stringers and 16,355 psi for the inner stringers. After lengthening the cover plates eighteen inches for the tapered cut-off detail and rounding off the length to the nearest one-half foot, the resulting maximum design live (H-20) and dead load stress at the end of the cover plates varies from 12,300 psi to 12,700 psi for the inner stringers and 13,300 psi to 13,600 psi for the outer stringer.

Several interesting phenomena occurred during the recording of the data for random traffic. Though these phenomena were not unexpected, they were interesting enough that a brief study of the extent and cause of them was undertaken. They were all a part of the dynamic response of the structure and were a function of the speed and position of the vehicle on the structure. The study of these dynamic characteristics was done with a known load operating at a known speed along a given lane of the bridge slab.

The Standard Truck

The standard truck was used as the controlled loading to study the effects of speed and position of the vehicle on the bridge structure.

Speed. Figure 9 shows the stress-frequency curves for the indicator gage on the inside stringer at the end of the long coverplate. The moving load for these curves was the standard truck. The only variable in the data used to construct these stress-frequency curves was the speed of the vehicle. The increased number of repetitions of a given stress is indicative of the increased vibration which accompanies an increase in speed. The increase in the ordinate of each curve is an indication of the amount of impact which resulted from the moving load. Although the curves show an increase in the repetition of stress as the speed increases, it is apparent that the speed which produces the maximum number of oscillations is not necessarily the maximum speed. The final answer as to the most critical speed was beyond the scope of this research, but it is believed that the maximum vibration for a given structure is a function of speed, length of truck, and continuity of traffic.

Position. The amount of vibration in the bridge structure is the determining factor in the amount of repetition of stress. It was found that in the bridge investigated, which has a 48 foot roadway, that the lane in which the truck was traveling vibrated less than the "unloaded lanes" (figure 10). In the stringer directly below the loaded lane and the stringer below the adjacent unloaded lane, the loaded stringer has the larger stress, however, the greatest number of repetitions in stress occur in the other stringer, although at a much lesser stress.

The position of the load used in the construction of these stress-frequency curves is shown in figure 11. One wheel passed directly along

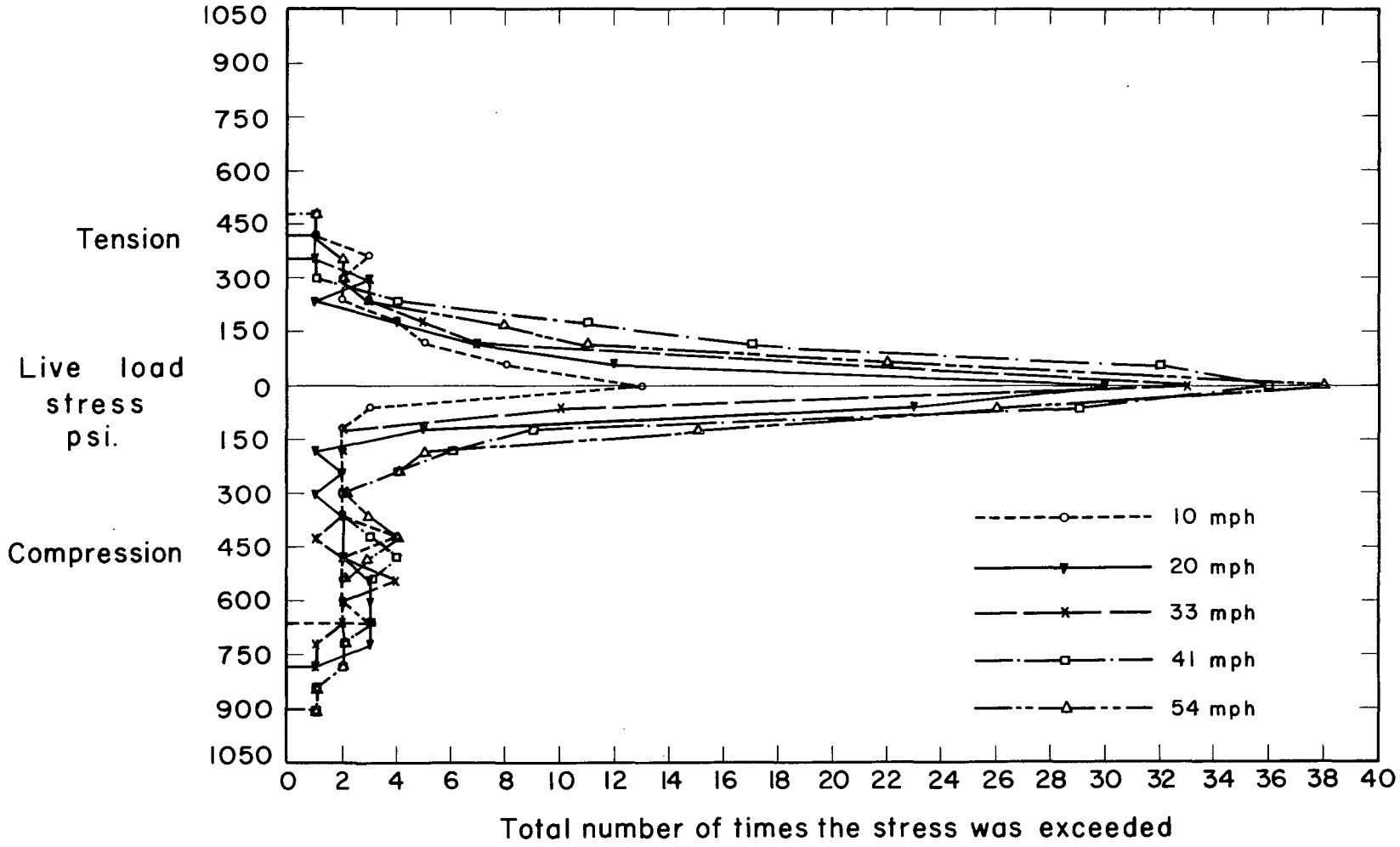

Figure 9. Effect of speed on stress frequency.

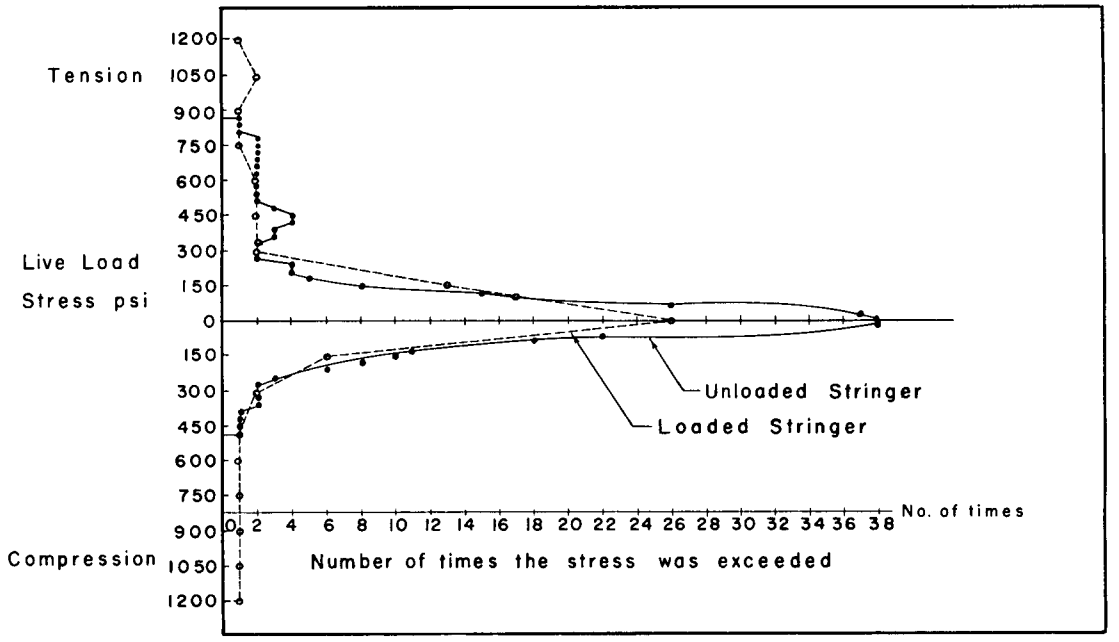

Figure 10. Stress frequency curve for loaded and unloaded stringers.

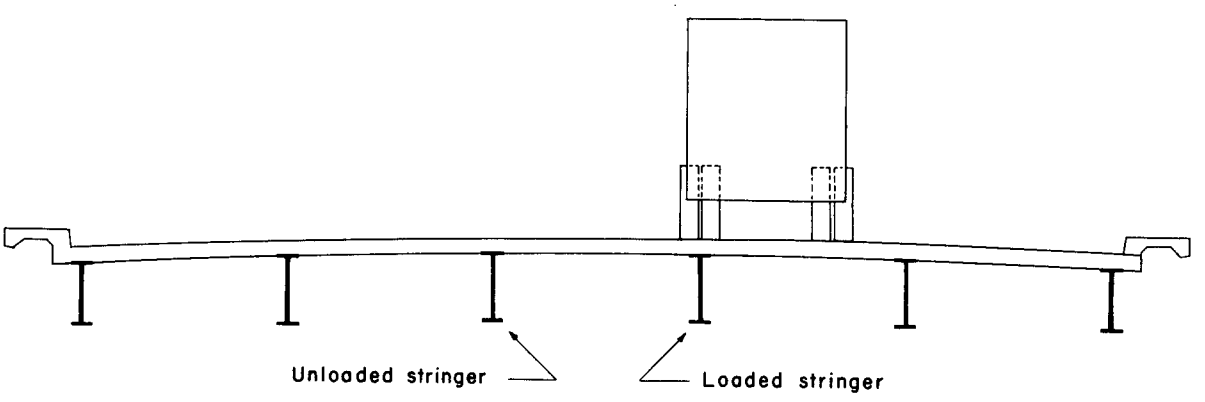

Figure 11. Position of the load with respect to the loaded and unloaded stringers.

the "loaded" stringer. The distribution of total live load to the "loaded" and "unloaded" stringers was approximately 37 and 14 percent respectively.

THE COMPOSITE SECTION

In the typical continuous stringer highway bridge the moment of inertia of the wide flange section and cover plates at the pier is approximately the same as the moment of inertia of the composite stringer. This leads to an often used simplified analysis of live loads which assumes that the moment of inertia is constant throughout the length of the bridge. This assumption could make a considerable difference in the calculated live load moments. Therefore, to evaluate the correctness of the uniform section assumption, the properties of the stringer cross-section were determined at three places along the bridge. These three sections are: a typical positive moment section, a section in which there are extreme reversals in moment, and a typical negative moment section (sections I, II, and III, figure 1).

All three sections are located in the exterior span of the three span bridge. Section I is located at point 0.4L of the end span from the abutment; this is approximately the point of maximum positive moment. Section II is located 17 feet from the pier and is just beyond the cover plate cutoff point. Section III is located 3 feet from the pier, near the point of maximum negative moment and yet away from the influence of the reaction and the pier diaphram.

Another purpose of investigating the properties of the stringer cross-sections was to evaluate the actual moments of inertia and section moduli of all the stringers at one section of the bridge. This was necessary before the experimental load distribution data could be reduced and compared with the design data.

It was found that the sum of the measured strains for all the stringers at the cross-section of section I was 200 micro in/in ± 5%, regardless of the lateral position of the load vehicle on the roadway. This seemed to indicate that the section moduli were the same for all the stringers and the lateral spreading of the load was not affected by the position of the load, or that these two factors combined so that the final result was a constant. To investigate the mechanics of the distribution of load more thoroughly, the neutral axes were determined for each of the stringers at this cross-section of the bridge. One half of the bridge was instrumented at section I for the determination of the neutral axes of the stringers. Five SR-4 strain gages were positioned on each steel stringer. One gage was located at the center of gravity of the rolled section, and the other four gages at the extreme fibers and the quarter points of the rolled section. The locations of the neutral axes were then used to determine the amount of concrete slab which was working compositely with the steel stringers. Since the roadway surface was spalled, the top 1/2 inch of the slab was disregarded in these calculations. The moment of inertia was then determined using the necessary amount of slab. A modular ratio of 10 was used in these calculations.

The experimentally located neutral axes varied considerably from the calculated location based on the specifications, and it did not depend on the load or the type of bending moment, either positive or negative. A number of readings were taken with different vehicles going in either direction across the bridge. The experimentally determined neutral axis varied less than four percent of the depth for any particular stringer.

Section I

At Section I, the point of maximum positive moment, the position of the experimentally determined neutral axis varied for the two inner stringers, although they are both 36 WF 194 rolled sections. This position of the neutral axis was, in both cases, closer to the wide flange centroidal axis than the calculated location based on specifications. This resulted in the stringer closest to the longitudinal center-line of the bridge using 35.0% less slab than allowed by the specifications. The location of the neutral axis for the outer stringer, a 33 WF141 rolled section, was found to be farther from the wide-flange centroidal axis than the calculated location based on specification. This indicates that the outer stringer has more slab acting compositely with the stringer than is available according to the specifications. Using only the roadway slab in the reduction of neutral axis data, the slab required by the outer beams exceeds the amount remaining after the portion needed by the inner beams is subtracted from the total roadway. A more realistic approach for justifying the position of the neutral axis in the exterior beam is the use of some portion of the sidewalk and curb in addition to the slab as the composite beam. This presents the problem of what amount of each of these parts to use in the composite beam. If only the curb directly above the roadway slab is used, 10 ft., 2 in. of roadway slab is required to complete the composite section. This is an unrealistic quantity of slab since the stringers are 9 ft., 4 7/32 in. center to center. This indicates that an arbitrary maximum amount of slab should be used with the sidewalk and curb. The limiting width of slab acting with the rolled section was taken as one-half the distance to the next stringer plus the overhanging slab under the curb. In addition to this slab, 22 1/2 inches of sidewalk curb was required by the experimentally

determined position of the neutral axis.

The moments of inertia of the composite stringers at section I resulting from these calculations were 27,050 in.^{4}, 26,580 in.^{4}, and 24,500 in.^{4} for the three stringers on one side of the longitudinal center-line (beginning with the outer stringer). The section moduli show more similarity than the moments of inertia. The composite section moduli are respectively, from outer to inner stringer, 856 in.^{3}, 892 in.^{3}, and 876 in.^{3} or a variation from the average of $\pm$ 2% (figure 12).

Section II

Section II, 17 ft., 0 in. from the pier, is near the dead load contraflexure point and is subjected to extreme variations in the live load bending moment. Because the section is just outside the cover plate cutoff point, the results indicate the effect of the cover plates on the neutral axis in an area where an abrupt change is theoretically indicated but actually incongruous. The position of the neutral axis of the outer stringer indicates that only a small portion of the sidewalk and curb acts in addition to the arbitrary maximum amount of roadway slab (the arbitrary maximum width for the slab extends to the midpoint between beams). The moment of inertia of the composite stringer is 22.9% less at this section than at section I. This is the result of lower position of the neutral axis which of course results in a smaller composite section. One factor affecting this is the size of the rolled section. The outer stringer changes from a 33WF141 to a 33WF152 at a splice on both sides of the pier. Thus, section II is a larger (33WF152) wide flange than section I. Thus, the neutral axis will move toward the center of gravity of the rolled section as this rolled section becomes larger. Also, the cover plates, which terminate nearby, have a tendency to bring the neutral axis closer to the centroid of the rolled

section. However, the extent of this effect is unknown.

The inner stringers at section II, both 36WF194 rolled sections, have neutral axes closer to the wide-flange centroidal axes than observed at section I. This resulted in an average reduction in moment of inertia of 10.2%. The position of the neutral axis was the same for both inner stringers at section II.

A comparison of the moments of inertia and section moduli of the stringers at section II shows a variation of $\pm$ 4.6% in the moments of inertia while the section moduli varied $\pm$ 9.2%. The moments of inertia are 20,830 in.^{4} for the outer stringer and 22,900 in.^{4} for the inner stringers. The section moduli are 712 in.^{3} and 856 in.^{3} for the outer and inner stringers respectively.

Section III

The third section at which the neutral axes were found was 3 ft., 0 in. from the pier. This section is near the point of maximum negative moment but should not be affected by the reaction of the pier or by the pier diaphram. The location of the neutral axis of the outer stringer at this point corresponds approximately to the location of the neutral axis at section II (at the end of the long cover plates). But, because of the cover plates, two plates on the top and bottom flanges, the required amount of composite concrete is increased, and, of course, the moment of inertia is greatly increased. The position of the neutral axis of the outer stringer required that more than all the sidewalk be used in addition to the maximum amount of roadway slab (the arbitrary maximum width of slab extends to the midpoint between beams). Therefore, in addition to all the sidewalk and curb 110.2 inches of roadway was used in the calculations. The resulting moment of inertia and section modulus of the outer beam were 44, 030 in.^{4} and 1,381 in.^{3} respectively.

The inner stringers at section III also exhibit a large amount of composite action. The inner stringer closest to the longitudinal center line required 80.6 inches of slab and the other interior stringer required 112.4 inches of slab. The location of the neutral axes at section III of the inner stringers corresponds approximately to the locations of neutral axes at section II. Again because of the cover plates, the size of the composite section is considerably greater. The moments of inertia for the two inner stringers are 48,040 $in.^4$ and 47,690 $in.^4$, the latter being the stringer closest to the longitudinal center line. The section moduli are 1,600 $in.^3$ and 1,680 $in.^3$, for these two stringers respectively.

The total width of roadway slab required at section III exemplifies the composite action situation in the section of negative bending. The total width of roadway required by all three stringers is 25 ft., 3 inches plus the sidewalk and curb. This required slab exceeds the total slab available by 10 inches over the entire width of the bridge. Thus, it is evident that composite action occurs at the pier, and this action should be considered in design if a true analysis is desired.

These neutral axes results are incomplete for the determination of the variations in cross-section along the entire length of the bridge. They do show, however, that the final composite cross-section varies greatly at different sections along the bridge stringers. The variations in moments of inertia and section moduli along the outer span of the three span bridge can be shown most clearly by reducing the actual values to unit values. Using the moment of inertia and section modulus of the outer stringer at section I as a base, the ratio of the values at sections II and III respectively to the values at section I are:

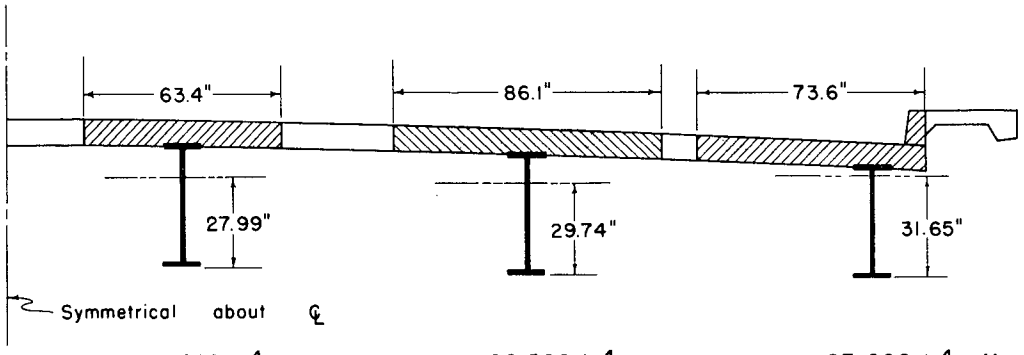

24,502 in.^{4} 876 in.^{3} | 26,580 in.^{4} 892 in.^{3} | 27,020 in.^{4} – Moment of inertia; 856 in.^{3} – Section modulus

Section I

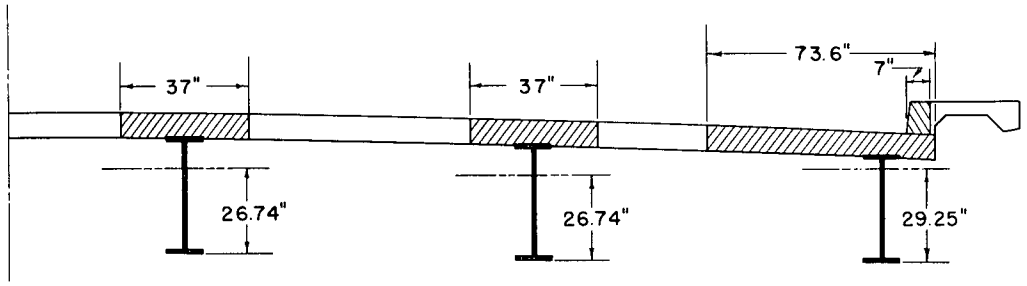

22,900 in.^{4} 856 in.^{3} | 22,900 in.^{4} 856 in.^{3} | 20,830 in.^{4} – Moment of inertia; 712 in.^{3} – Section modulus

Section II

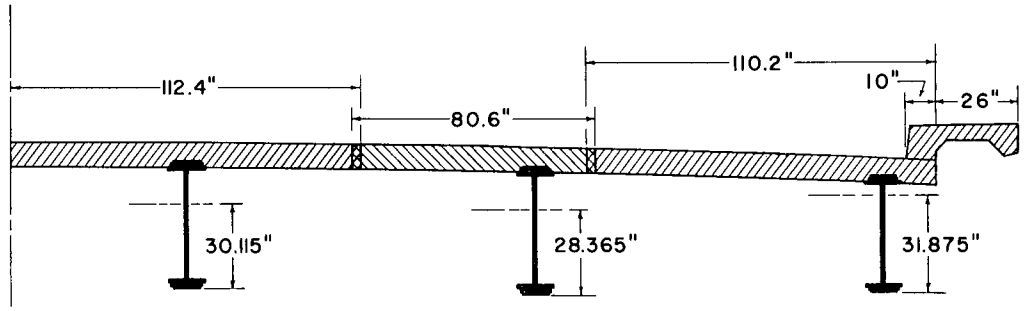

48,045 in.^{4} 1,600 in.^{3} | 47,693 in.^{4} 1,680 in.^{3} | 44,031 in.^{4} – Moment of inertia; 1,381 in.^{3} – Section modulus

Section III

Figure 12. A cross section of the bridge at sections I, II, and III showing the composite moments of inertia, section moduli, and the effective slab.

Ratio of Moments of Inertia

Stringer	Section I	Section II	Section III
Outer	1.0	0.77	1.62
Inner	0.981	0.846	1.77
Inner (closest to longitudinal center line)	0.906	0.846	1.76

Ratio of Section Moduli

Stringer	Section I	Section II	Section III
Outer	1.0	0.83	1.61
Inner	1.04	1.0	1.96
Inner (closest to longitudinal center line)	1.02	1.0	1.87

The moment of inertia of the composite outer stringer is 8% smaller than the moment of inertia of the composite inner stringer even though the moment of inertia of the outer stringer rolled section is an average of 35% smaller than the moment of inertia of the inner stringer rolled section. The difference is in the amount of composite slab assumed by each of the respective stringers and the sidewalk and curb which act with the outer stringer.

LOAD DISTRIBUTION

Of particular interest to the design engineer is how the vehicle loads are distributed to the supporting beams. A number of research programs have been conducted on this subject [3, 4, 5]. The results of some of these projects are in the recent revision of the American Association of State Highway Officials design specifications. Although the primary intent of this research was not to evaluate load distribution to the longitudinal stringers, this

problem was encountered in this research when an analysis of the experimental stresses was made.

The complexity of the slab-stringer type bridge does not lend itself conveniently to an exact solution. The slab, which is the roadway, also acts as an integral part of the longitudinal stringers. The continuity of slab over the stringers and the unequal deflections of the stringers combine to make load distribution a function of many variables. Therefore, the results contained in this report are for one bridge and cannot be considered conclusive for all slab-stringer bridges.

The 48 foot wide roadway has resulted in longitudinal distribution of the concentrated wheel loads over a very wide area. This yields a total moment at any one cross-section of the bridge which results from a relatively concentrated load, if a stringer is directly beneath the wheels, and a distributed load on the other stringers. This distributed load is probably a function of the lateral distance from the wheel to the stringers.

The moments in the bridge stringers at section I were determined by measuring the outer fiber flexural strains at that cross-section and multiplying each strain by the modulus of elasticity of steel and the section modulus of the corresponding beam. The total moment at this section is then the sum of these moments.

Since the section moduli of the stringers at section I are almost equal, and since the sum of the experimentally measured strains for all the stringers at section I are also constant regardless of the lateral position of the load, as previously hypothesized, the lateral spreading of the load was not affected by the lateral position of the load on the roadway.

It was found that regardless of the lateral position of the loading vehicle on the roadway, that the total moment of all the stringers at section I varied only $\pm$ 2.2% from an average of 424 kip ft. for the vehicle

traveling toward the abutment (west to east) and only ± 1.5% from an average of 431 kip ft. for the vehicle traveling toward the pier (east to west). These moments occur with the rear axle of the vehicle at section I.

The theoretical moment at section I which results from the standard vehicle traveling toward the abutment, assuming a constant cross-section and no longitudinal distribution, is 550 kip ft. The corresponding total experimentally determined moment of 424 kip ft. is 77.1% of this theoretical value. Similarly, the theoretical moment at section I resulting from the standard vehicle traveling toward the pier, again assuming a uniform cross-section and no longitudinal distribution, is 564 kip ft. The experimental moment of 431 kip ft. is 76.5% of this theoretical moment. This percentage corresponds very closely with the previous one.

The difference between the experimental and theoretical moments is the result of the longitudinal distribution of load and the variation in cross-section. The longitudinally distributed load extends over the entire length of the stringer farthest from the wheel load and over a smaller portion of a stringer closer to the wheel load, and like the variations in cross-section, this would tend to decrease the positive moment.

By using the individual moment of each stringer as a percent of the total moment, the variation in the lateral distribution of load can be determined for the stringers. This assumes the moment diagram for all the stringers are identical in shape, similar to the design assumptions. Figure 13 shows the static load distribution at section I (approximately the point of maximum positive bending moment) as a percent of load carried by each stringer. The cross-section of the bridge is shown at the top of the graphs, and the position of the truck is indicated on each particular graph.

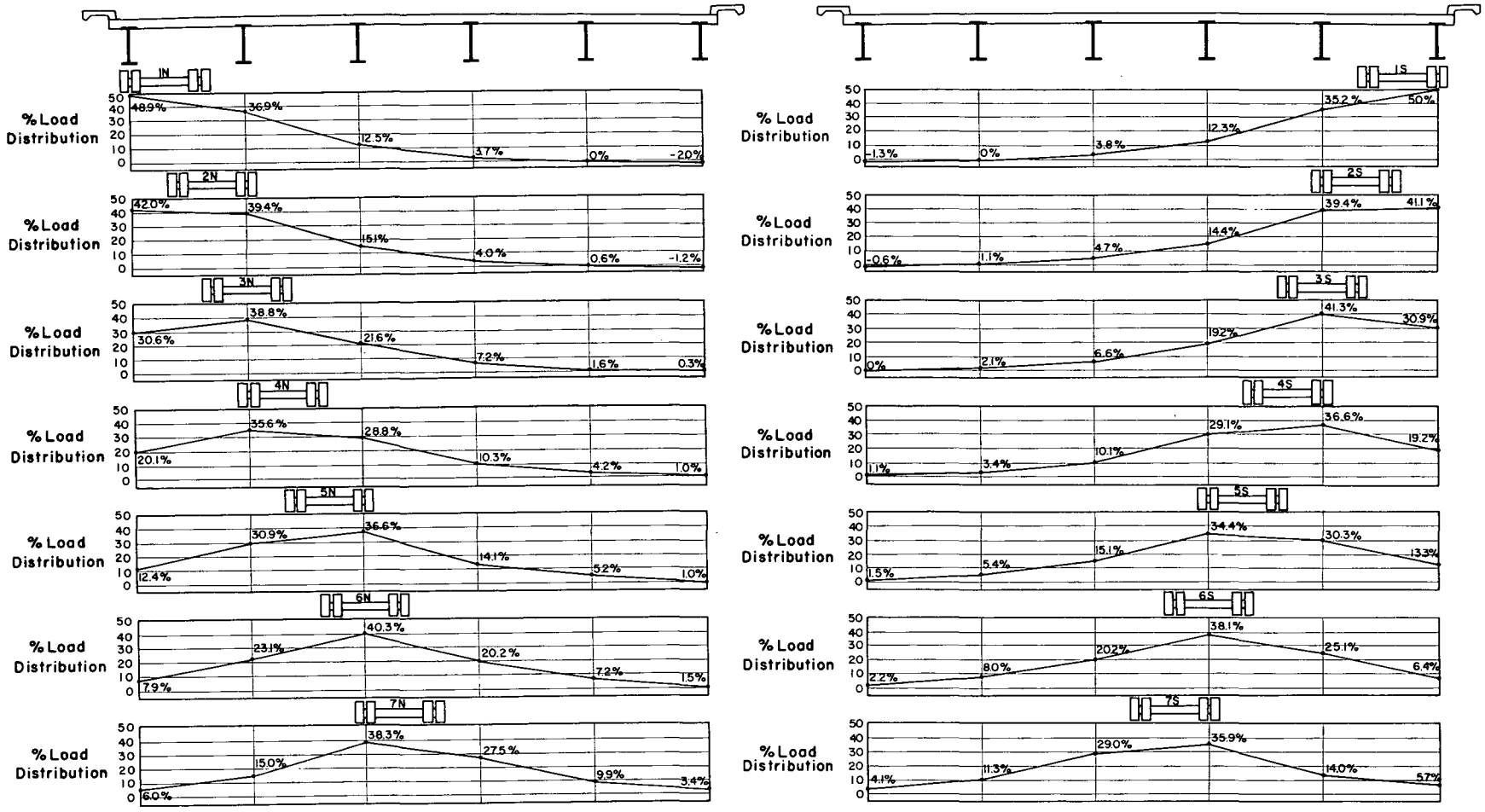

Figure 13. Static load distribution at section I.

In obtaining the maximum distribution of load to the various stringers, the static load distribution curves were used with the assumption that superposition is valid [6]. The largest number of standard vehicles which contribute to the load in each respective stringers were superimposed on the bridge roadway. Each vehicle was limited in its lateral movement to the width of its lane less approximately two feet for clearance. This could be accomplished by using the experimental lane data without any need for interpolation. Three trucks were used for the outer stringers and four vehicles were used in the computation of the maximum load on the inner stringers.

By loading lanes 1-S, 5-S, and 6-N the roadway is loaded to produce the greatest load in the outer stringer while keeping the trucks approximately within two feet of the edge of their respective lanes (figure 13). To improve the accuracy of the results the percent distribution values were averaged with the corresponding values for the other outer stringer using lanes 1-N, 5-N, and 6-S. The resulting average load distributed to an outer stringer is 64.15% of a standard vehicle. This corresponds to a wheel load distribution factor of 1.283.

The lanes loaded to produce the largest load in the inner stringer immediately adjacent to the outer stringer are lanes 2-S, 5-S, 2-N, and 6-N for this stringer on the south and 2-N, 5-N, 2-S, and 6-S for this stringer on the north (figure 13). Averaging these two values, the average percent of a standard vehicle distributed to each of these stringers is 78.45%. This corresponds to a wheel load distribution factor of 1.569

The lanes loaded to produce the largest load in the inner stringer closest to the longitudinal center-line are lanes 2-S, 6-S, 6-N and 2-N for both the stringers on the north and on the south of the longitudinal center-line. The average percent of a standard vehicle distributed to each of these stringers is 78.5%. The wheel load distribution factor for these stringers is therefore 1.57, which is very close to the wheel load distribution factor for the other inner stringers.

These distribution factors are for approximately 77% of a unit vehicle load as a result of the variation in cross-section and the longitudinal distribution. A comparison of these values can now be made with the A.A.S.H.O. design specification load factors.

The specifications require that a load factor of S/5.5 be used in determining the fraction of a wheel load applied to an interior (inner) stringer. For this bridge the load factor for an inner stringer is 1.70.

The fraction of a wheel load applied to the outer stringers by the A.A.S.H.O. specifications shall not be less than "The reaction of the wheel load obtained by assuming the flooring to act as a simple beam between stringers" or the fraction of a wheel load found by

$$\frac{S}{4.0 + 0.25S} \qquad 6' \leq S \leq 14'$$

The first criteria results in a load factor of 1.06 while the second criteria results in a load factor of 1.475. Thus, the second load factor governs.

Investigating the problem of load distribution further, another method of analysis was used to determine the theoretical amount of wheel load distributed to the outer stringers. This is a method which makes use of the formula usually associated with eccentric column analysis [7].

The formula is

$$f = \frac{P}{A} \pm \frac{Pey}{I}$$

or

$$W_n = I_n \left[\frac{P}{\Sigma I} \pm \frac{PeC_n}{\Sigma Iy^2} \right]$$

in which

P = Total load

e = Eccentricity of load

C_n = Distance of Nth girder from centroid of I's

ΣI = Sum of I's for all girders

ΣIy^2 = Sum of the moments of inertia of I's

I_n = Moment of inertia of Nth girder

W_n = Load carried by Nth girder

This formula is used by the Iowa State Highway Commission to determine the amount of load distributed to the outer stringers. A unit moment of inertia is assumed for each stringer so that it is not necessary to approximate the relative sizes of stringers prior to the analysis. It was found that for the bridge tested, the experimental moments of inertia varied less than 6% at the 0.4L point (section I). Thus, the use of unit moments of inertia is a good approximation for this bridge. By placing three vehicles in the position for a maximum load on an outer stringer and using the above method of analysis, a theoretical design load factor of 1.64 is found. This value corresponds to the loading which produces the largest experimental load. However, a design loading of four vehicles would be used by the Iowa State Highway Commission, and this results in a design load factor of 1.452 for the outer stringer.

The Effect of Impact on Load Distribution

It has been suggested by one author that the increase in stress due to impact for highway bridges "might be almost any value between 10 percent and 200 percent of the amount given by the specifications" and that an over-all impact factor might be apportioned to the stringers individually [7]. This suggestion and others dealing with impact seem to indicate that the simplicity with which impact is handled in design, has resulted in large inequities in the actual stresses produced in different type bridges under similar loads [8]. From the data obtained during this research an analysis of impact and the effect on the distribution of loads may be made.

Moving load tests were performed using four of the fourteen test lanes. Speed increments of 10 mph were used up to the maximum speed obtainable from the vehicle (approximately 50 mph). The vehicle used was the standard H-20 truck. The stress resulting from the moving vehicle was obtained as a continuous strain time record. A similar record of the vehicle moving slowly across the bridge had been obtained. This was considered the static stress with no impact. The effect of the dynamic loads is considered to be the variation from this static strain record. This variation appeared as a transient vibration superimposed on the static strain record. The amount of the impact resulting from this moving load cannot be considered to be the maximum. The maximum amount of impact for this bridge would probably result from a truck-trailer combination with the maximum trailer length. This is a surmise in a relatively unexplored area that needs further research. The importance of the data presented here is not in the quantitative but instead in the qualitative aspect. The way in which the impact affects the distribution of load and the way in which the impact *per se* is distributed is the objective of this data.

The distribution of load to the various stringers for a vehicle traveling on the experimental lanes at various speeds is shown in figure 14. At the top of the graph is the bridge cross-section with the vehicle position located. Each part of the graph indicates the load distribution for a different speed. The solid line indicates this dynamic load distribution for the vehicle at section I, and the dotted line represents the value obtained from the static tests at the same section. The static test values were determined from the strain time curve obtained by the vehicle moving slowly across the bridge. This is the same static load distribution curve shown in figure 13. The resulting variations between the dynamic and static load distribution curves are very small.

Shown in figure 15 is the impact or increase in stress which is shown as a percentage ratio of the dynamic moment to the static moment. This value for the individual stringers is shown beneath the respective stringers. The total impact in the bridge cross-section is a percentage ratio of the total dynamic moment to the total static moment in the bridge cross-section. The total impact is shown at the right of each graph. The individual impact values vary considerably and in some cases are less than one hundred percent, or less than the static value. This indicates that the dynamic moment was smaller than the static. Also, the impact ratio for some stringers is shown as infinity which results from a zero static live load moment. The total bridge impact values also vary considerably, but their tendency is to increase as the speed increases. The vehicle is shown on the bridge cross-section at the top of the figures in the position for which the underlying series of dynamic results were obtained.

The impact values obtained for the individual stringers cannot be compared with the total bridge impact values. These two values vary considerably and are the basis of many contradictory conclusions.

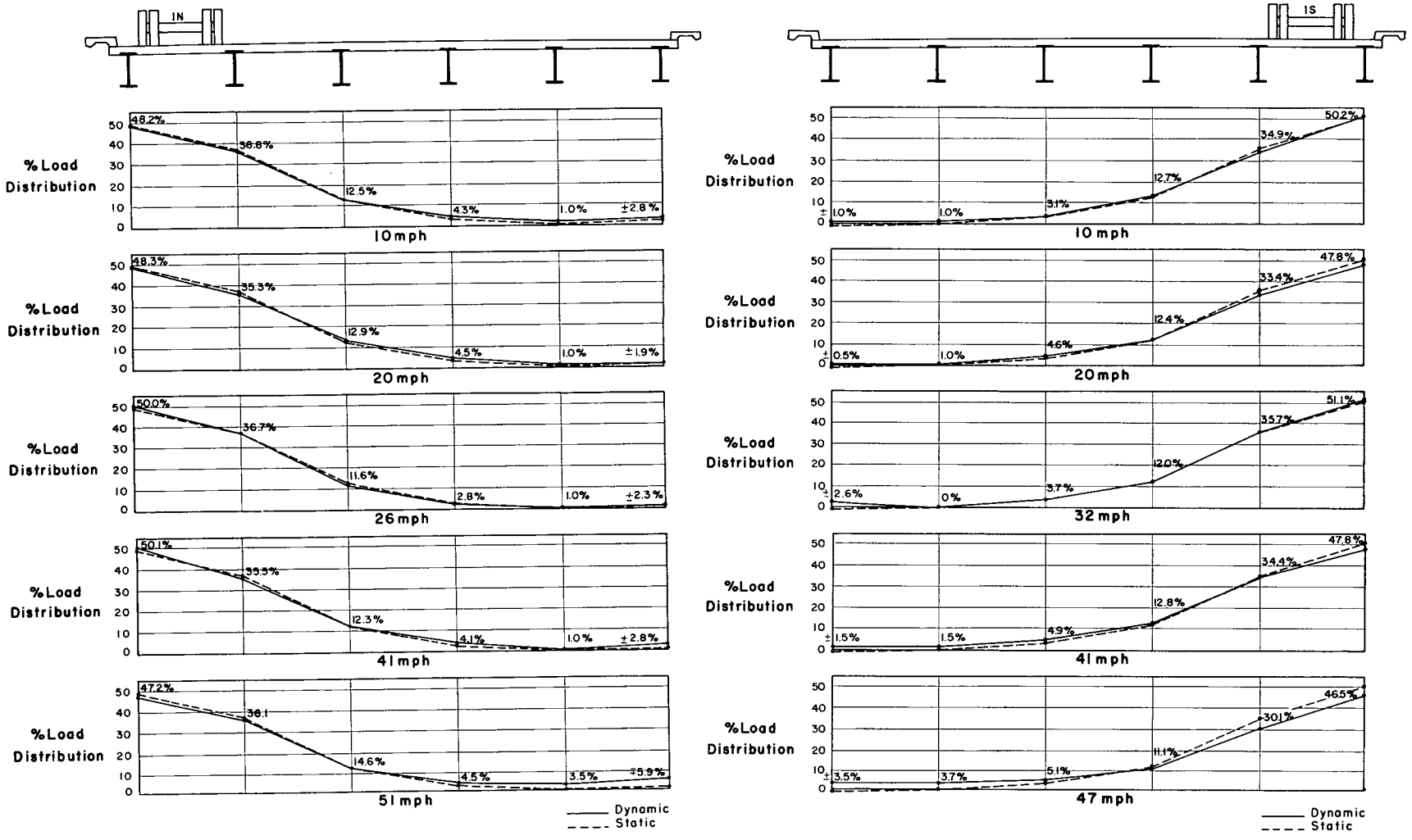

Figure 14. The effect of speed on the distribution of load; the percent figure applies to the dynamic load only.

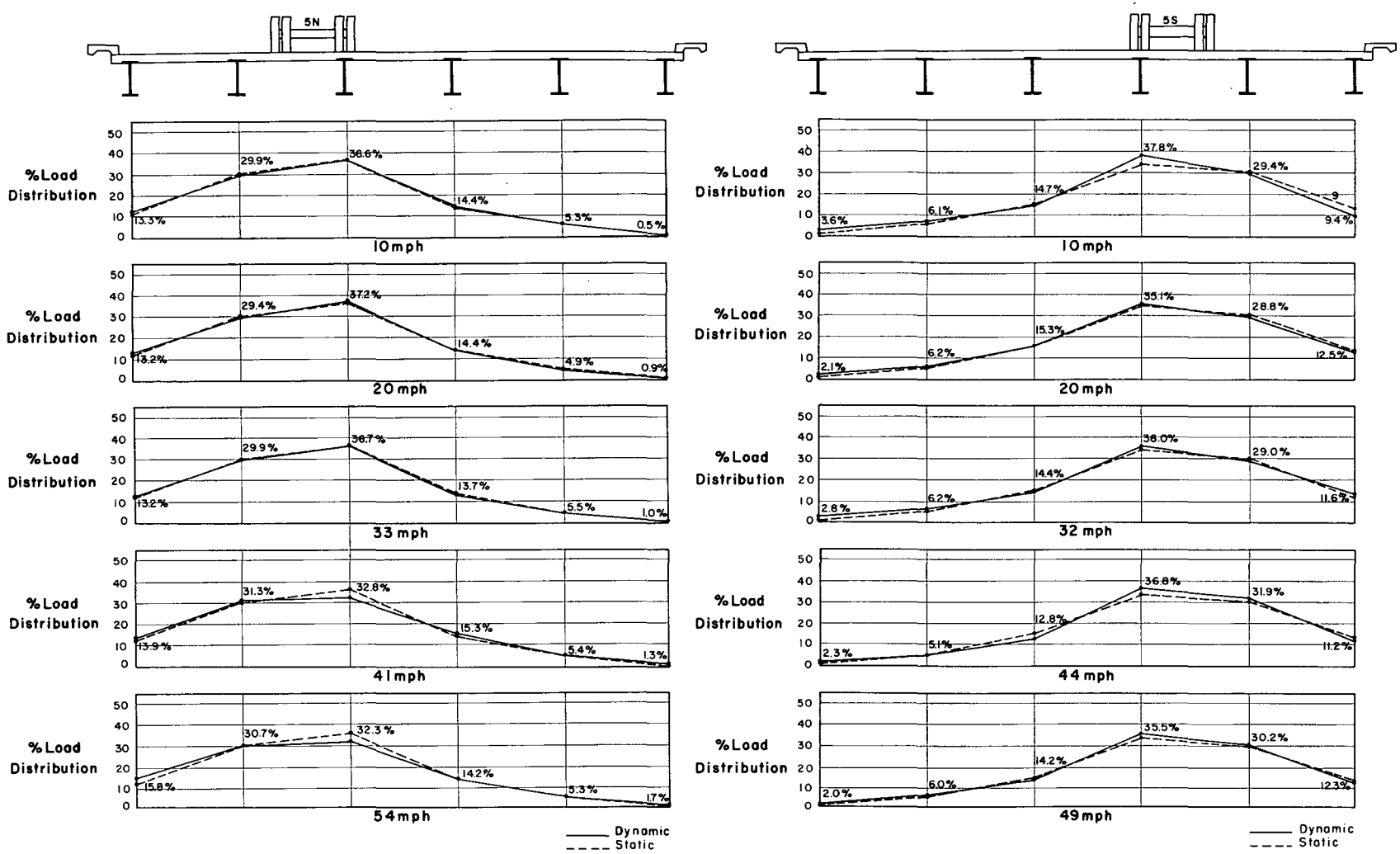

Figure 14. Continued.

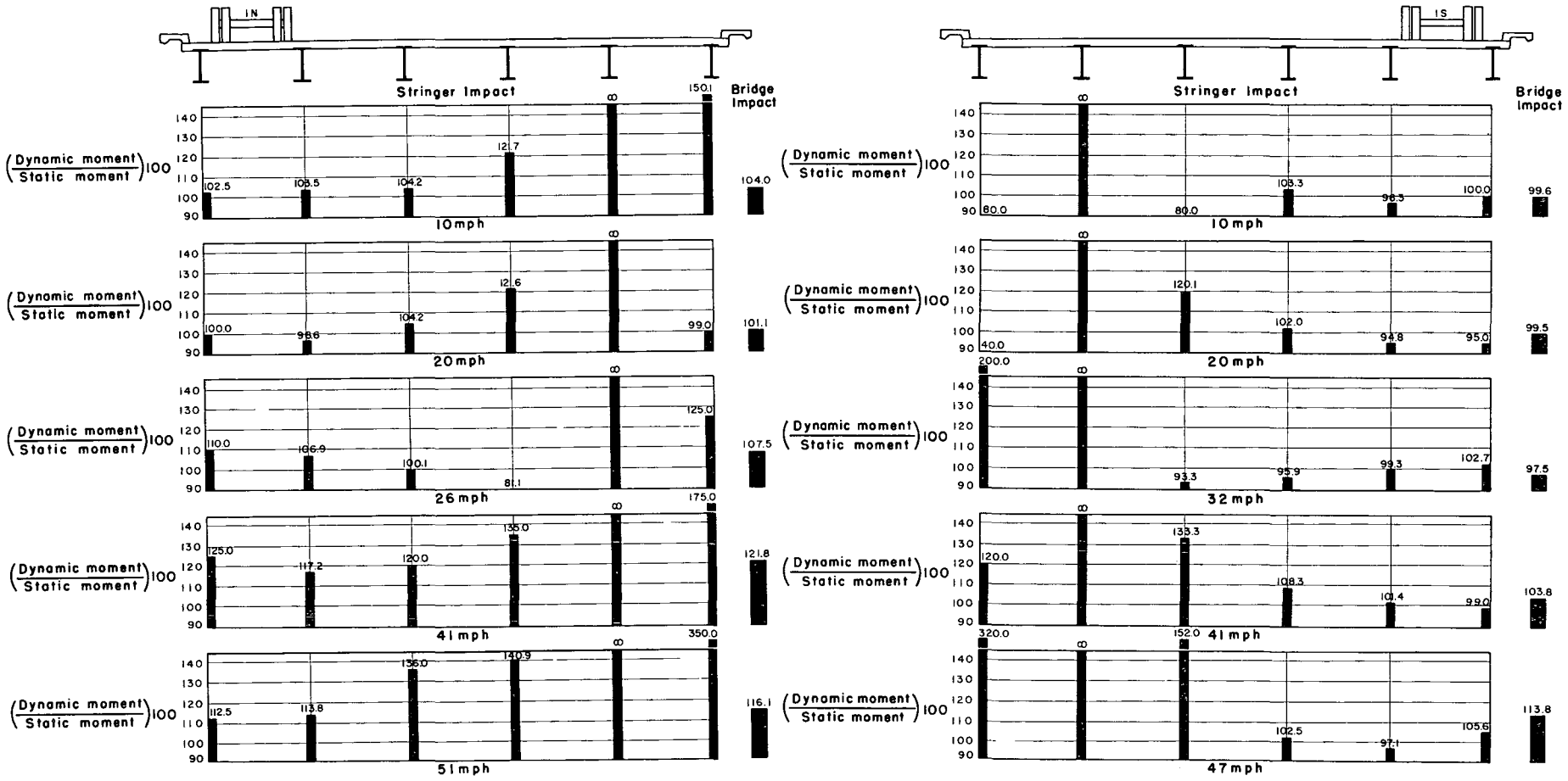

Figure 15. Percent impact for each stringer and for the whole bridge.

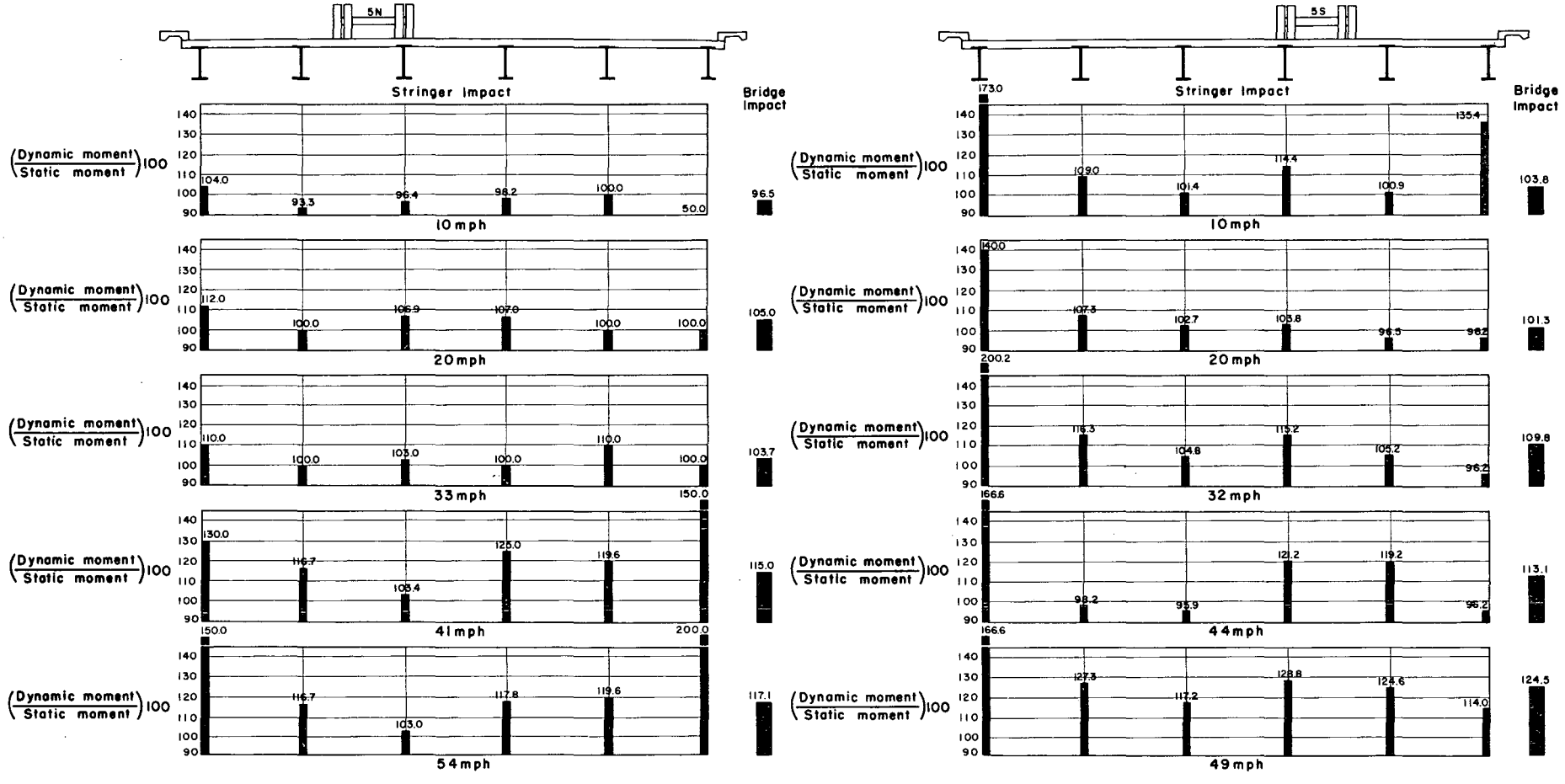

Figure 15. Continued.

SUMMARY AND CONCLUSIONS

The structure tested in this research program was a three span continuous composite steel stringer bridge typical of the type used by the Iowa State Highway Commission on primary and interstate highways. Some detail changes have been made by the I.S.H.C. bridge design section in this type since this bridge was built. However, the results obtained in this research are at least qualitatively applicable, and some are quantitatively applicable to the continuous composite steel stringer bridges being designed.

STRESS FREQUENCY AND FATIGUE

The stress frequency curves obtained in this research indicate that the number of cycles of repetition is large, although the corresponding stress is rather small. Approximately the largest repeated live load stress produced was 1,800 psi and this was not repeated more than nine times in the 7 1/2 hour sampling period. The stringers with the largest dead load stress which were subjected to this maximum repeated live load have a stress variation pattern of $4{,}500 \pm 1{,}800$ psi, or a maximum stress of 6,300 psi. and a minimum of 2,700 psi. A comparison of this data with the results of other fatigue tests [1] can be made to determine if the fatigue strength of these cover plate termination areas might be critical. Using a summation [2] of fatigue data for "Beams with partial length cover plates attached with continuous fillet welds", a fatigue strength of $11{,}500 \pm 2{,}500$ psi. is indicated for 2,000,000 cycles of zero to maximum stress. Assuming the ultimate strength of structural steel is 60,000 psi, and using Goodman's equation, an indication is obtained of how the fatigue strength of "Beams with partial length cover plates attached with continuous

fillet welds" compares with the experimental results of the stress frequency data for the structure tested. By using the more critical fatigue strength of 9,000 psi, (11,500-2,500) and assuming that the dead load stress level is 4,200 psi, the repeated amplitude of stress for fatigue to be critical is ± 4,425 psi. Alternately, assuming a repeated amplitude of stress of ± 1,800 psi. and the same fatigue strength as above, the dead load stress level for critical fatigue is 37,300 psi. Because the dead load stress level for most bridges will correspond closely to the value for the bridge tested, and because it is not likely that the dead load stress level will be increased in the future, a closer look at the critical repeated amplitude is necessary.

From the experimental results, it is possible to obtain an average repeated amplitude of ± 5,890 psi. by placing eighteen H-20 trucks on the test structure. This does not include the dynamic effect that such a combination of vehicles might produce but on the other hand it requires a spacing of vehicles of 7.33 feet. This hypothetical case shows that it is possible for the critical fatigue amplitude to be exceeded, although the possibility of it occurring often enough to produce a fatigue failure, is, at the present, absurd.

The previous simple calculations seem to indicate that the cover plate termination regions investigated are not critical due to fatigue considerations. However, the fatigue strength based on the Illinois fatigue tests should not be applied without some concern about the difference between the fatigue tests and the actual bridge stringers which are being compared. The comparison of the experimental fatigue results with the actual stress-frequency of the bridge stringers is based on a phenomenon first studied by Wohler, [9] and later formulated by Gerber and Goodman. All these results are based on the idea that the range of stress

necessary to produce failure decreases as the mean stress increases. This permits a comparison of the zero to maximum stress condition of the experimental fatigue results with a mean stringer stress of 4,200 psi. plus or minus the live load stress amplitude in the bridge stringer. However, other investigators have shown that there is no general law connecting the mean stress and the stress range. It is necessary, therefore, to obtain experimental fatigue data for the range of stress at the critical regions of the bridge stringers before their fatigue life can be determined with any certainty. For additional accuracy in the correlation of experimental fatigue tests with the actual bridge stringer data, the experimental stress cycle during the fatigue test should be varied periodically to correspond with the actual stress variations. This fatigue test, with varying amplitudes of stress, would estimate service life under service stresses. To correlate this experimental fatigue test with the actual service stress condition, the previously determined stress frequency curve is converted to a stepped curve with a logarithmic scale, and this is converted, in turn, to the variable stress fatigue program required for testing.

Each variable stress fatigue program is one series of stress cycles. These stress cycles are continued, one series after another, until failure occurs. In a second program all the stresses are multiplied by a constant factor, thus a curve similar to the usual endurance curve is obtained which relates stress level to the life of the specimen. This curve could be used to determine an allowable design stress, after the application of a safety factor.

A stress frequency curve in figure 7 is converted to a stepped curve in figure 16, and the resulting variable stress fatigue program is in figure 17. Only with the results from a variable stress fatigue experiment based on a program similar to that in figure 17 will the designer ever know

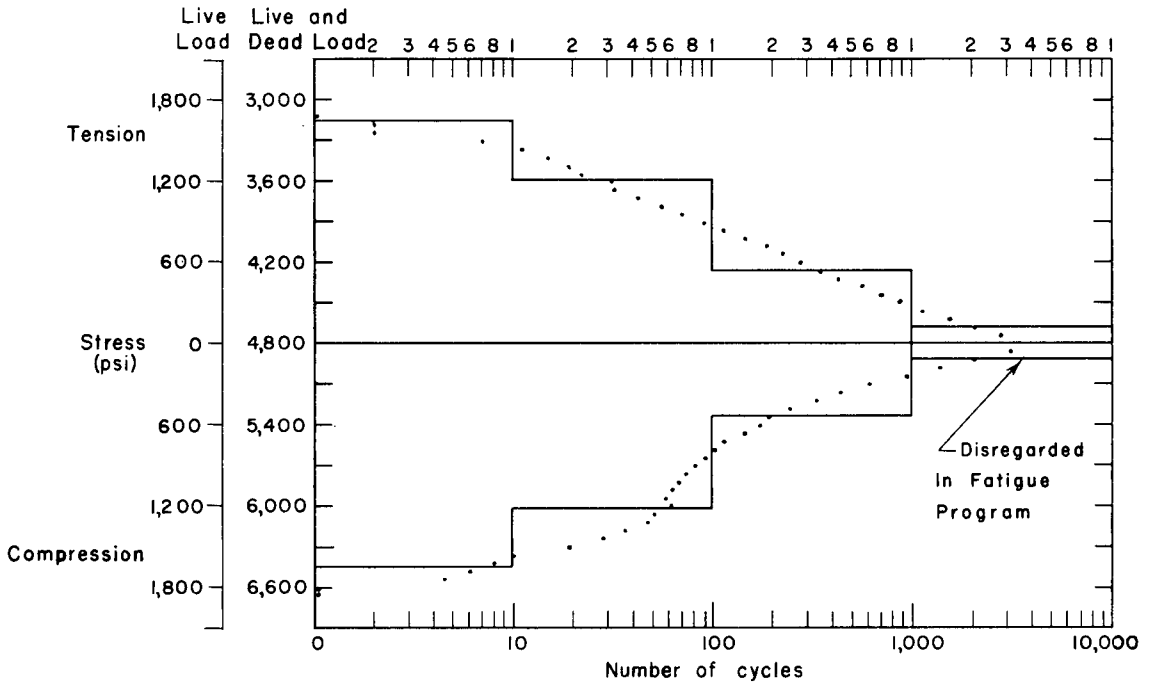

Figure 16. A stepped stress frequency curve for the cover plate termination detail of the outer stringer in the end span.

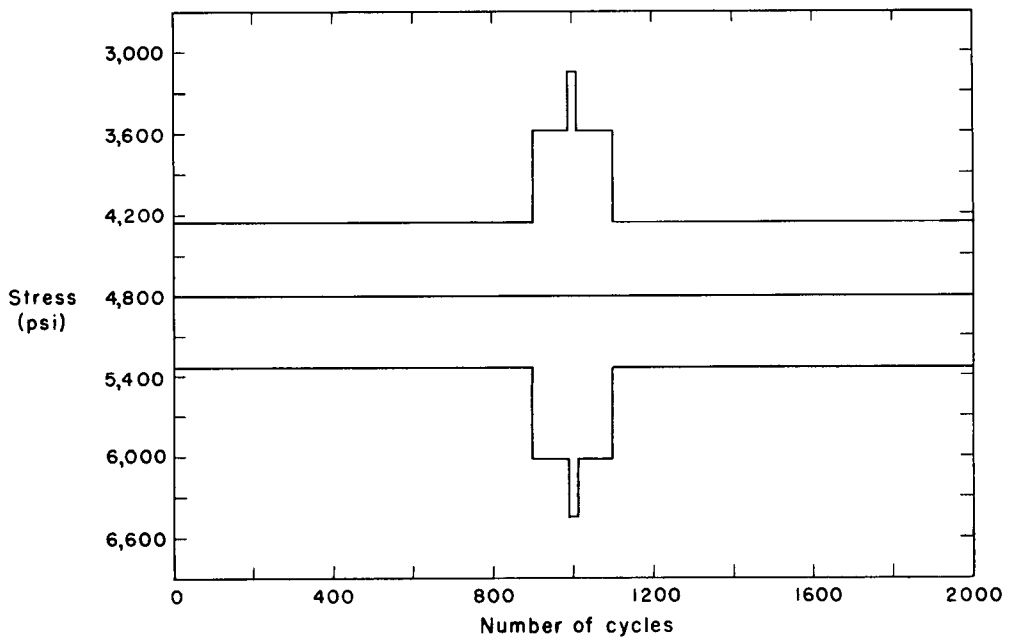

Figure 17. A stress fatigue program for the outer stringer in the end span.

whether bridge structures have a finite fatigue life, at which point they will require extensive repair, or whether the cover plate termination stresses are ultra conservative.

VARIATIONS IN CROSS SECTION

It has been shown that there is composite action even in cross sections subjected to negative bending. This occurs even though a maximum live load tensile strain of 60 micro in /in was experimentally determined in the extreme top fiber of the roadway slab. This corresponds to a stress of approximately 180 psi. Therefore, it is not unrealistic to assume that there is composite action all along the stringer.

It might be possible, by using this composite action judiciously to attach the cover plates to the lower flange only or even to omit them entirely. For instance, if the same amount of slab acted compositely with an inner stringer without cover plates as with an inner stringer with cover plates, the composite moment of inertia would exceed by 10%, the theoretical moment of inertia of the non-composite wide flange with cover plates.

The data and results for the composite cross-sections also indicate that the assumption that the final moments of inertia of the stringers are constant throughout the length of the bridge is very much in error. The positive moment regions have composite action as assumed in design, and the resulting moments of inertia correspond closely to the theoretical moment of inertia of the wide flange sections with cover plates and no composite action. However, the composite action at the supports increases the moment of inertia 148% for the outer stringers and 85% for the inner stringers. Therefore, the final ratio of the moment of inertia at the negative moment section with respect to the moment of inertia at the positive moment section is an average of 1.79 for all the stringers. This

indicates the error in the live load moments which are based on a constant moment of inertia.

These data also indicate the large increase in the moment of inertia of the outer stringer due to the sidewalk and curb. A comparison between the non-composite outer and inner stringers at the pier shows that the numerical moment of inertia of the outer wide flange is sixty-five percent of the moment of inertia of the inner wide flanges. When composite action is considered, the moment of inertia of the outer stringer is only eight percent less than the value of the moment of inertia of the inner stringers. Similarly, at the positive bending section the composite action limited by specifications results in the moment of inertia of the outer section being sixty percent of that of the inner section. The actual composite sections, including the effect of the sidewalk and curb on the outer stringer, results in the moment of inertia of the outer stringer being approximately six percent more than that of the composite inner stringers. It is clear from the above discussion that the stringers tend to use the amount of slab necessary to equalize the moments of inertia at the various cross-sections.

LOAD DISTRIBUTION

The load distribution data show, quite clearly, the error introduced by assuming that no longitudinal load distribution occurs. The error is increased further by the variation in moments of inertia. The large composite moment of inertia in the negative bending area (section III) tends to increase the negative moment at the pier. It is possible for this to decrease the positive moment at section I three to five percent. Therefore, since the experimental moment was found to be twenty-three percent less than the theoretical moment, it can be assumed that about twenty percent of the reduction in the experimentally determined moment can be attributed to longitudinal distribution of the wheel loads.

If the longitudinal distribution of load is disregarded, the lateral load distribution factors agree rather closely with the values specified by the American Association of State Highway Officials. The experimental lateral load distribution factors of 1.57 for the inner stringers is 7.6% less than the A.A.S.H.O. design load factor of 1.70. Similarly, the experimental load distribution factor of 1.283 for the outer stringer is 13% less than the A.A.S.H.O. load factor of 1.475. The other method which makes use of the eccentrically loaded column formula results in a lateral load distribution factor, as used by the Iowa State Highway Commission, of 1.452 7. Here, the experimental value of 1.283 is 11.6% less than this design value. Thus, the relatively small irregularities in lateral load distribution are overshadowed by the initial assumption that there is no distribution of longitudinal load.

IMPACT

The data indicate the dynamic moments and how they are distributed in the bridge cross-section. The stringers with the largest load percentage-wise have an increase in moment; however, the increase in percentage is often larger in the stringers with less moment. This results from the vibrational amplitude of the stringers depending more on their mass than on their static load. Therefore the moment resulting from the vibration of the stringers with a smaller static moment shows the largest increase in percentage.

It is apparent that the distribution of load undergoes no large change as a result of the vibrational impact. The greatest change occurs when the truck is in the outer lane and produces an upward or negative moment in the extreme opposite outer stringer. The dynamic effect of the truck is a vibration superimposed on the static load distribution. Thus, when the vibrational amplitude causes the greatest increase in moment, the sign of

the dynamic vibratory moment is opposite to the sign of the static moment in this outer stringer. The result is an apparent decrease in moment in the extreme opposite outer stringer and therefore a small change in the load distribution percentages. Even so, the dynamic load distribution percentages were always within five percent of the static load distribution percentages. As a result, the change in the dynamic load distribution was always well within the difference between the experimental and design load distribution factors.

The total impact in the bridge shows an increase with speed, the amount of impact depending upon whether or not the amplitude of vibration coincides exactly with the maximum moment in the bridge stringers. The maximum total bridge impact measured was 24.2%. This corresponds to a specification impact value for the outer span of 23.2%. The similarity of these two values is not indicative of the usual maximum bridge impact percentages.

The individual stringer impact values depend upon the amplitude of the vibratory moment and the static moment level. For the most heavily loaded stringers, the maximum impact values are somewhat similar to the maximum bridge impact values. The largest impact value in a heavily loaded stringer is 28.8%. This is not unlike the similar total bridge maximum percentages.

It is difficult to determine what value of impact might be suitable for design. The two values compared in this study are the individual stringer impact percentages and the total bridge impact percentages. These two values vary considerably and would probably vary more if a more critical, in terms of vibration, truck trailer combination had been used.

REFERENCES CITED

1. Wilson, W. M., Flexural fatigue strength of steel beams, Eng. Exp. Sta., Bul. 377, University of Illinois, Urbana, Illinois. 1948.

2. Hulsbos, C. L., and Hanson, J. M., Factors influencing the fatigue strength of steel beams in highway bridges, Progress Report To Iowa Highway Research Board, Iowa Eng. Exp. Sta., Iowa State University, March, 1958.

3. Siess, C. P., and Veletsos, A. S., Distribution of loads to girders in slab and girder bridges: Theoretical analyses and their relation to field tests, Highway Research Board Bul. Rep. 14-B., Washington, D. C., 1952.

4. Holcomb, R. M., Distribution of loads in beam and slab bridges, Iowa Highway Research Board, bulletin No. 12, Ames, Iowa. 1959.

5. Newmark, N. M., Design of I-beam bridges, Proceedings of A.S.C.E. March, 1948.

6. Caughey, R. A., and Senne, J. H., Distribution of loads in beam and slab bridge floors, Final Report to Iowa Highway Research Board, Iowa Eng. Exp. Sta., Iowa State University, Sept., 1959.

7. Wise, J. A., Dynamics of highway bridges., Proc. Highway Res. Board, Vol. 32, pp. 180-7 1953.

8. "Vibration and stresses in girder bridges", Highway Research Board Bul. 124, Washington, D. C., 1956.

9. Timoshenko, S., Strength of materials, part II, Advanced theory and problems, D. Van Nostrand Co., Inc., New York, 1956.

Table I. Strain-frequency data — number of times the strain was exceeded.

Strain micro in / in	Stringer					
	Outer		Outer-Inner		Inner	
	Center span	End span	Center span	End span	Center span	End span
58	1			4		
56	1	1		8		
54	1	2		13		
52	1	2		11		
50	1	7	2	22		
48	3	11	6	25		
46	3	15	11	33		1
44	4	19	16	38		1
42	6	22	17	43	1	2
40	6	31	23	47	2	5
38	6	32	30	56	2	5
36	9	42	37	58	3	5
34	10	55	46	67	3	6
32	12	70	63	77	5	6
30	17	90	75	90	7	8
28	28	113	79	105	9	10
26	32	145	83	111	11	13
24	41	186	92	130	14	30
22	51	226	103	143	16	40
20	56	275	110	161	21	56
18	64	342	121	191	30	71
16	80	423	130	239	41	91
14	97	541	129	303	62	130
12	126	692	148	398	86	194
10	174	869	163	556	115	289
8	251	1120	214	739	161	423
6	390	1536	443	1051	243	618
4	651	2058	577	1625	422	958
2	1228	2734	958	2558	754	1384

Strain micro in / in	Stringer					
	Outer		Outer-Inner		Inner	
	Center span	End span	Center span	End span	Center span	End span
2	1171	3089	1001	2655	779	1289
4	739	2035	605	1700	558	888
6	446	1383	412	1158	420	634
8	309	930	331	767	303	458
10	232	609	271	562	244	393
12	185	438	224	391	193	325
14	138	329	174	318	147	276
16	117	244	150	265	127	221
18	97	192	122	206	103	183
20	89	171	102	170	94	162
22	80	144	95	142	83	134
24	76	112	92	112	68	104
26	73	102	85	107	50	100
28	71	91	82	99	42	89
30	64	81	81	93	33	75
32	55	74	74	87	27	63
34	51	69	67	87	23	54
36	38	63	60	86	20	42
38	33	59	54	80	15	29
40	29	61	45	77	10	21
42	21	50	36	68	9	14
44	18	47	31	68	5	13
46	12	36	25	56	4	9
48	12	28	15	56	4	6
50	8	19	14	48	3	3
52	6	10	9	42	3	
54	5	8	9	39	3	
56	3	6	7	32	3	
58	3	4	5	20	3	
60		2	4	14	2	
62			3		2	

Table II. Impact strain (micro in/in) at section I.

Loading lane	Speed mph	Stringer					
		Outer N	Outer-Inner N	Inner N	Inner S	Outer-Inner S	Outer S
5-N	10	26	56	70	27.5	10	1
5-N	20	28	60	77.5	30	10	2
5-N	33	27.5	60	75	28	11	2
5-N	41	32.5	70	75	35	12	3
5-N	54	37.5	70	75	33	12	4
5-S	10	5.2	12.0	29.4	75.5	57.5	19.2
5-S	20	4.2	11.8	29.8	68.5	55	25
5-S	32	6	12.8	30.4	76	60	25
5-S	44	5	10.8	27.8	80	68	25
5-S	49	5	14	34	85	71	30
1-S	10	-2	2	6	24.8	65	100
1-S	20	-11	2	9.0	24.5	64	95
1-S	32	-5	0	7.0	23	67	100
1-S	41	-3	3	10	26	68.5	99
1-S	47	+8	8	11.4	24.6	65.5	105.5
1-N	10	102.5	75	26	9	2	-6
1-N	20	100	70	26	9	2	-4
1-N	26	110	77.5	25	6	2	-5
1-N	41	125	85	30	10	2	-7
1-N	51	112.5	82.5	34	11	8	-14

Table III. Static stain (micro in/in) at section I.

Loading lane	Stringer					
	Outer N	Outer-Inner N	Inner N	Inner S	Outer-Inner S	Outer S
1-S	-2.5	0	7.5	24	67.5	100
1-N	100	72.5	25	7.4	0	-4.0
2-S	-1.2	2	9.2	28	75	81.5
2-N	85	76.5	30	8.0	1.2	-2.4
3-S	0	4	13	38	80	62.5
3-N	61	74	42	14	3.0	+0.5
4-S	2	6	18	52	64	36
4-N	40	68	56	20	8	2
5-S	3	11	29	66	57	26
5-N	25	60	72.5	28	10	2
6-S	4	14	36	77	44	15
6-N	18	45	80	40	14	5
7-S	8	21	55	68	26	11
7-N	12	30	75	54	19	68